Anal Bioanal Chem (2016) 408:49–65
DOI 10.1007/s00216-015-9043-1

REVIEW

Advances in explosives analysis—part II: photon and neutron methods

Kathryn E. Brown[1] · **Margo T. Greenfield**[1] · **Shawn D. McGrane**[1] · **David S. Moore**[1]

Received: 25 August 2015 / Accepted: 10 September 2015 / Published online: 7 October 2015

Abstract The number and capability of explosives detection and analysis methods have increased dramatically since publication of the Analytical and Bioanalytical Chemistry special issue devoted to Explosives Analysis [Moore DS, Goodpaster JV, Anal Bioanal Chem 395:245–246, 2009]. Here we review and critically evaluate the latest (the past five years) important advances in explosives detection, with details of the improvements over previous methods, and suggest possible avenues towards further advances in, e.g., stand-off distance, detection limit, selectivity, and penetration through camouflage or packaging. The review consists of two parts. Part I discussed methods based on animals, chemicals (including colorimetry, molecularly imprinted polymers, electrochemistry, and immunochemistry), ions (both ion-mobility spectrometry and mass spectrometry), and mechanical devices. This part, Part II, will review methods based on photons, from very energetic photons including X-rays and gamma rays down to the terahertz range, and neutrons.

Keywords Explosives detection · Trace analysis · Explosives · Improvised explosives · Instrumentation · Reviews

Explosives glossary

AN	Ammonium nitrate
ANTA	3-Amino-5-nitro-1,2,4-triazole
DNB	Dinitrobenzene (isomers 1,3-DNB and 1,4-DNB)
DNT	Dinitrotoluene (isomers 2,4-DNT and 2,6-DNT)
FOX-7	1,1-Diamino-2,2-dinitroethene (DADNE)
HME	Homemade explosive
HMTD	Hexamethylene triperoxide diamine
HMX	Octagen; octahydro-1,3,5,7-tetranitro-1,3,5,7-tetrazocine
IED	Improvised explosive device
Picric acid	2,4,6-Trinitrophenol
NG	Nitroglycerine; nitro; glyceryl trinitrate; RNG; trinitroglycerine
NTO	Nitrotriazalone
PETN	Pentaerythritol tetranitrate; 2,2-bis[(nitroxy)methyl]-1,3-propanediol; dinitrate
RDX	Cyclonite; hexogen; hexahydro-1,3,5-trinitro-1,3,5-triazine
Semtex	Composition of PETN (or RDX and PETN) with heavy oils and rubbers
TATP	Triacetone triperoxide
Tetryl	Methyl-2,4,6-trinitrophenylnitramine
TNT	2,4,6-Trinitrotoluene; 2-methyl-1,3,5-trinitrobenzene

ABC Highlights: authored by *Rising Stars and Top Experts*.

✉ David S. Moore
moored@lanl.gov

[1] Los Alamos National Laboratory, Shock and Detonation Physics Group, Los Alamos,, NM 87545, USA

Introduction

Part I provides a more complete introduction to this review [1]. This part, Part II, will cover many of the newest and most capable explosives detection and analysis capabilities that use photons to interrogate the sample. Also included are methods using neutrons. We include several exciting new stand-off detection developments at distances of 100 m and beyond. Our principal focus will be on archival scientific literature, rather than vendor information, in order to concentrate on the scientific principles and advances rather than commercial off-the-shelf (COTS) embodiments, except in selected cases. The recent shift in predominant usage from military

explosives to homemade explosives (HME) has driven substantial changes in detection methods, particularly to differentiate threats from benign usage (e.g. farming) of HME components.

Methods using ionizing radiation or neutrons

X-ray diffraction

X-ray diffraction (XRD) of a sample provides crystalline structure information. It is a promising non-invasive, non-contact method to detect and identify liquid and solid materials [2, 3]. In energy-dispersive (ED) XRD, a polychromatic X-ray beam is used to probe the photon–matter interactions of coherent scattering in the sample. An energy-resolved detector at a fixed scattering angle measures the material-specific spectrum. The specificity of the spectrum results from the atomic planar spacing (d) and radiation wavelength (λ) of the material according to Bragg's law ($2d\sin\theta = n\lambda$, n is an integer). Alternatively, as in angle-dispersive X-ray diffraction (AD-XRD), one can keep λ fixed and vary θ [4]. These isomorphic detection techniques are most applicable to TSA or detection portals, because the equipment is non-portable due to size and shielding requirements.

Advantages of XRD over typical X-ray imaging techniques are covered in Well's comprehensive review from 2012 [3]. X-ray diffractive-imaging devices are commercially available, and their intrinsic features necessary for detecting solid and liquid explosives and inert materials are summarized by Harding [5]. Much work over the past five years has been on improving detectability through combining detection techniques [4, 6], analysis methods [7], and optimization of X-ray geometry [8–12] and detector geometry [11]. Combining AD-XRD and ED-XRD with a pixelated energy-resolved detector requires no moving parts and short acquisition times (~1 s), when merged with principal component and discrimination analysis, to differentiate between inert materials and explosives including Semtex and ammonium nitrate emulsions [6]. X-ray emission spectroscopy for future trace and small-scale-bulk detection is also being investigated, but to a much lesser extent [13–15].

Neutron activation and gamma emission

Active neutron-interrogation methods are used to identify the relative chemical content of specific elements (N, O, Cl, and H) via their characteristic gamma-ray emission, neutron scattering, and neutron absorption. Abnormally high nitrogen content is typically used as a detection flag for an explosive. Neutron activation works well for high-nitrogen explosives, but not all explosives are nitrogen based, e.g., the homemade explosives TATP and potassium chlorate plus sugar. Two main advantages of using neutron activation are the ability of neutrons to pass through high-atomic-number materials, for example metals, and the specificity to differentiate between organic and inorganic materials. The largest disadvantages are that neutron sources produce harmful radiation doses if not shielded properly or at the correct stand-off, and neutron interrogation can cause unwanted material activation.

There are five main neutron-activation interrogation techniques: thermal-neutron analysis (TNA), fast-neutron analysis (FNA), pulsed fast–thermal neutron analysis, fast-neutron elastic scattering (NES), and neutron transmission/fast neutron radiography. A 2014 review by Whetstone and Kearfott describes the basic principles behind each of these interrogation techniques and emphasizes their advantages and disadvantages, and gives an overview of the different neutron sources currently used for each technique [16]. An alternative detection method suggests using gamma rays to induce neutron scattering for detection [17].

Advances in this field focus on fusion of different techniques, advances in neutron sources in terms of energy and portability, and increases in detection sensitivity. FNA, TNA, and dual X-ray imaging were combined to analyze ratios of four common elements (Cl, H, Fe, and N). Use of different ratios of the elements (e.g., N–H, Cl–H, and Cl–N) was found to reduce the false alarm rate, and use of eight detectors in front and eight behind a container enabled location of a suspect material (Fig. 1) to within an area 0.4×0.4 m [18]. A tabletop 10 Hz thermal-neutron generator for gamma spectroscopy has been developed in France using a dense-plasma-focus technique [19]. Scintillator development for TNA gamma-emission detection was found to increase medium-to-large antitank-landmine detection to a depth of 30 cm and horizontal displacement of 30 cm, and enable detection of moderate-to-large ammonium nitrate-based IEDs (improvised explosive devices) in culverts [20]. Further experiments on IEDs and UXO (unexploded ordinance) suggest the gamma-emission count time depends on a combination of the soil moisture, cladding thickness of the explosive containment, and, to a lesser extent, the explosive composition [21]. Recent work by Batyaev measured and calculated gamma-emission receiver operating characteristic (ROC) curves on explosives (TNT, Tetryl, NG, and RDX) and benign materials, and revealed that it was possible to estimate ROC curves [22].

Terahertz methods

Terahertz spectroscopy and imaging

Terahertz (THz) spectroscopy (the spectral region is usually defined as frequencies from 0.5 to 10 THz, or wavenumbers from 15 to 300 cm^{-1}) and other long-wavelength spectroscopies (e.g. millimeter wave, GHz) probe the low-energy modes of molecules and longer-range intramolecular modes,

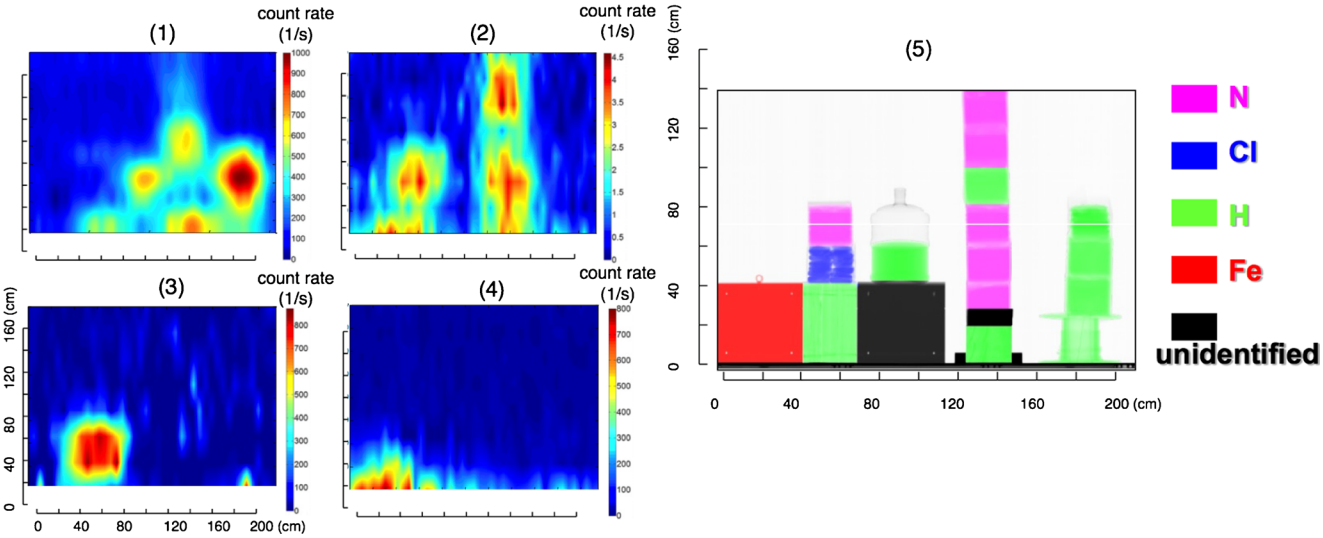

Fig. 1 Two-dimensional TNA elemental distribution of (**1**)hydrogen, (**2**)nitrogen, (**3**)chlorine, (**4**)iron, and (**5**)the combined X-ray image with elemental distribution. From Ref. 18, used with permission

yielding another set of molecular "fingerprints" for explosives detection. One promising attribute of THz spectroscopy is its ability to penetrate and detect non-metallic items, which is of benefit for detecting hidden or concealed objects. There is still a great deal of research being performed on obtaining the spectral signatures of different conventional and homemade explosives, and developing signal-processing techniques for both spectroscopy and imaging schemes. There are few THz detection papers containing quantitative analytical metrics, for example detection limits. The selectivity of the method is discussed in several papers, especially where it involves THz spectral signatures and their variation with sample type or matrix.

A common technique for THz spectroscopy is time-domain spectroscopy (THz TDS), a pump–probe method. A THz pump pulse (generated by an ultrafast laser) is sent through a sample to a detector, where it is combined with a shorter probe pulse from the laser. The THz electrical field can be recorded over a period of time, and can be Fourier transformed to a frequency spectrum. A great deal of research has been performed on the spectral signatures of explosives and related materials through THz TDS, including the conventional molecular explosives RDX, HMX, PETN, and simulant molecules [23–28]. Likewise, the spectral signatures of explosive mixtures and plastic compositions have been studied [26–33]. Additionally, spectral signatures of homemade explosives and related materials have been analyzed [34–36]. Using THz TDS for stand-off detection, where the operator is physically separated from the sample, has also been investigated [25, 31].

There are several challenges associated with THz spectroscopy for explosives detection, including interference from barrier or concealment materials (envelopes, clothing, etc.), surface roughness of the samples, and water vapor or humidity present in the air [30, 37]. Many researchers have addressed these challenges through developing methods to separate spectral fingerprints of explosives from barrier materials [30, 31, 38–40], and signal-processing algorithms to compensate for water-vapor absorption [32].

THz imaging has been suggested to be a more viable option for explosives detection than spectroscopy, although subject to similar challenges [37]. Two common techniques in recent THz imaging research are passive imaging, where the system detects naturally occurring radiation in the THz frequency range, and THz reflection imaging, where chemical identification is possible. The research on passive imaging has largely focused on image processing for high-resolution images. Trofimov et al. [40–42], along with collaborators in China [43], have developed several sets of spatial filters to apply to the obtained images to detect hidden objects. The challenge of surface roughness in THz imaging was addressed by Zurk and coworkers by a novel three-dimensional imaging technique through a synthetic aperture and by other methods [44–48]. Research to both detect and identify explosive objects has also been performed by several groups. Sleiman et al. used THz TDS for chemical mapping of RDX, PETN, and RDX–PETN mixtures [28]. Startsev et al. used a tunable optical parametric oscillator (OPO) to frequency raster-scan several explosives; the imaging analysis assessed the chemical composition of the materials studied (Fig. 2) [49]. Palka et al. compared the THz transmission spectra of explosives by THz TDS and an OPO-based system [50].

Researchers have coupled THz spectroscopy and imaging to other technologies. Carriere and coworkers [51–53] combined THz with Raman spectroscopy (THz-Raman) for extremely low frequency (~5 cm^{-1}) Raman measurements of

explosives. Lu et al. used a flexible tube-lattice fiber probe combined with THz TDS for THz hyperspectral imaging [54]. Perov et al. developed a new THz imaging scheme based on a backward-wave oscillator and heterodyne detector to detect concealed objects [55]. Simoens et al. developed a microbolometer-array prototype for explosives detection at two different frequencies [56, 57]. Bolduc et al. used a microbolometer-based THz imaging camera to detect a concealed plastic knife [58].

Vibrational and electronic spectroscopies

Infrared

Infrared (IR)-absorption, reflectivity, and attenuated-total-reflection (ATR) spectroscopies are powerful methods of explosive identification and detection via measurement of the vibrational spectrum. Portable devices that measure ATR spectra of unknown materials for identification by library matching are available from several commercial sources. ATR avoids the sample preparation traditionally involved in transmission IR measurements. Because infrared penetration depth for neat materials is on the order of a micrometer, trace amounts of solids or liquids (e.g., ng to μg) can be measured if they can be placed in contact with the ATR prism. Stand-off methods retain this sensitivity to trace residues while avoiding sampling.

Passive stand-off IR can use the thermal emission spectrum for identification. Long-wave infrared (LWIR) at 8–14 μm wavelength is emitted as thermal radiation from a sample that is modulated by the spectrally dependent emissivity. This signal is typically detected by HgCdTe-based sensors or microbolometer arrays through a Fourier-transform infrared (FTIR) interferometer [59]. Coupled with an infrared-sensitive focal-plane array detector, FTIR hyperspectral imaging is capable of detecting and identifying trace amounts of explosives on surfaces (at ~μg cm^{-2} levels) in 30 s [60–62]. LWIR can be used for thermal imaging without spectral resolution as a simpler, but less selective, means of identifying spatial anomalies in an environment that may be hazardous [63]. LWIR systems are also often sensitive to mid-wave IR (MWIR) light in the wavelength range down to 3 μm.

Active stand-off IR involves illumination with either a thermal source or a laser. Although diffuse scattering of thermal IR sources off the sample can aid in spectral acquisition [59, 60, 64], the collimation and power on-target for laser sources is far greater. Femtosecond optical parametric oscillators [65] and tunable carbon dioxide lasers [66] have been used as spectroscopic IR sources, but most research is currently focused on illumination by tunable quantum cascade lasers (QCLs). Active QCL illumination coupled with array detectors enables hyperspectral imaging that can match the spectrum of residues with library spectra of explosives (Fig. 3) [67–70]. The backscattering collected is a strong function of the angle of incidence, but the contrast in spectral features has been observed to remain with orders of magnitude less signal than specular reflection [64, 71]. QCLs have the resolution required to measure gases, as has been established for stand-off diffuse reflection [72] and headspace-monitoring cavity ringdown spectroscopies [73]. Multiple QCLs can be chained together to increase the spectral coverage [74].

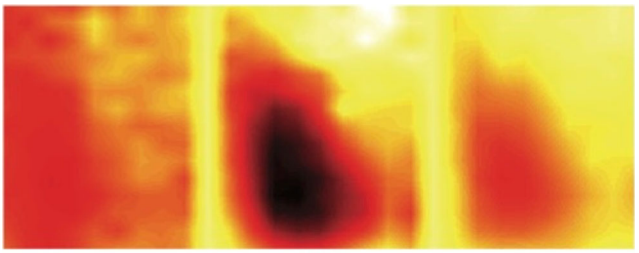

Fig. 2 Raster-scanned THz images of RDX concealed in a paper envelope with OPO tuned to 0.77, 0.83, and 0.90 THz. 0.83 THz is the frequency at the RDX resonance peak of width (FWHM Gaussian fit) 0.13 THz. From Ref. 49, used with permission

It should be noted that IR spectra measured in emission or backscattering geometries often look different from those measured by transmission or ATR. The particle size, shape, and environment can cause peaks to look absorptive, dispersive, or intermediate between the two [75, 76]. This is a fundamental physical property that must be accommodated in spectral-library-match algorithms.

Short-wave IR (SWIR) in the range 900–2500 nm offers more penetration ability than visible light and less expensive, more sensitive array detectors than are available at LWIR and MWIR. Whereas molecular vibrations absorb in the MWIR and LWIR, overtone (excitations of multiple vibrations) absorptions can be observed in SWIR. The spectroscopic determination of materials is less decisive, but the experimental implementation is simpler, smaller, and less costly. These advantages have motivated numerous implementations of SWIR hyperspectral imaging for explosives detection and identification. Discrimination among similar explosives imaged in handprint residues has been achieved [77, 78]. A dual SWIR and Raman hyperspectral imager on an unmanned ground vehicle was revealed to enhance explosive discrimination by coupling both methods [79]. A supercontinuum extending from 1300–4300 nm was used to measure diffuse reflectance spectra of several HE over a range extending from SWIR to MWIR [80].

Ultraviolet–visible

Detection and identification of explosives on the basis of reflectivity in the ultraviolet-to-visible ranges have not been as thoroughly researched as other methods. Because the underlying physics relies on electronic absorptions that are typically broad and indistinct, selectivity is not expected to be nearly as

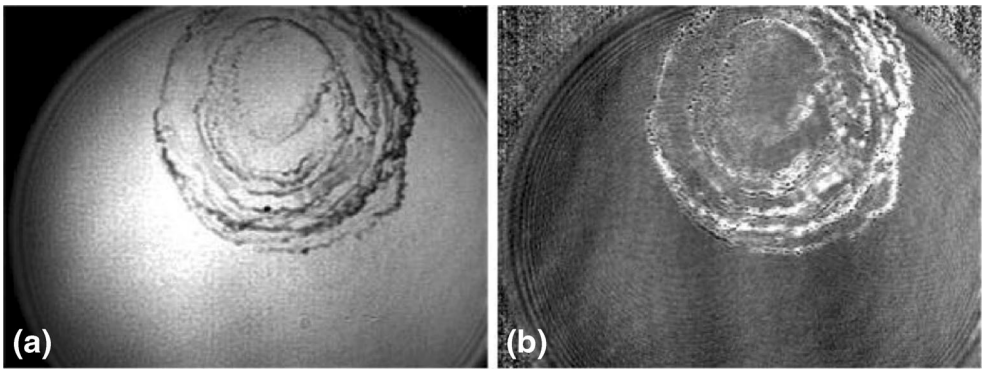

Fig. 3 Active hyperspectral imaging of an RDX residue using QCL illumination and an uncooled microbolometer camera. (**a**) Brightfield image. (**b**) Difference image showing bright areas of RDX residue caused by preferential absorption when compared with an off-absorption wavelength. Reprinted with permission from Ref. 69. ©2010 SPIE

high as for vibrational spectroscopy. Despite these difficulties, differential hyperspectral imaging [81, 82] under active illumination in the 200–500 nm range has been used to achieve a limit of detection (LOD) of 100 ng for TNT with selective ROCs [83].

Luminescence

Traditionally, chemiluminescence-based explosives detectors consist of a polymeric fluorophore that has some binding selectivity toward the explosive molecule [84]. Once bound, the fluorescence is quenched. This method has been used commercially in the Fido® detector (FLIR Systems, Inc.). Recent research into chemiluminescence explosives detection has focused on novel fluorescent materials and other luminescence schemes, including electrochemiluminescence and upconversion luminescence.

Novel materials for chemiluminescence-based explosives detectors include metal–organic frameworks (MOFs) and a variety of polymer and photonic crystal films. Hu et al. published an excellent review on the mechanisms of and research into metal–organic frameworks for small-molecule detection [85]. Xu et al. developed a nanoscale MOF to detect nitroaromatics in ethanol [86], and Wu et al. used a MOF for carbon disulfide and nitrobenzene detection [87]. Ma et al. [88] developed a U-bent PMMA optical fiber coated with a porous fluorescent polymer that experienced quenching with TNT (LOD: 10 ng mL^{-1}) and DNT. Sun et al. exploited nanostructure in a polystyrene–pyrene film, creating a fluorescent polymer with self-assembled nanopores to detect DNT vapor [89]. Ma et al. observed varied luminescence responses for different nitroaromatic explosives in an organic–inorganic hybrid ultrathin film: quenching for nitrobenzene and dinitrobenzene, an increase in fluorescence from DNT and TNT, and a fluorescence red-shift from picric acid [90]. Li et al. exploited the optical properties of an inverse-opal photonic crystal, a repeating structure consisting of spherical voids. The photonic crystal was coated with a fluorescent molecule, and was enhanced by the photonic crystal. The fluorescence was quenched with TNT [91]. Li et al. developed a sensor array to detect H_2O_2 as an indicator of TATP using CeO_2 nanoparticles. The nanoparticle membranes had a catalytic effect on luminol–H_2O_2 chemiluminescence. The system had a LOD of ~30 μg mL^{-1} [92].

Much attention has been given to ruthenium compounds, especially tris(bipyridine)ruthenium(II), $Ru(bpy)_3^{2+}$, as chemiluminescent materials for use in electrochemiluminescence (ECL)-based explosives detection. The reduction of TATP [93–95], RDX [96], or TNT [97] forms species that react with $Ru(bpy)_3^{2+}$, which generates ECL (Fig. 4). Ni et al. obtained a LOD of 0.7 mg mL^{-1} [97] TNT with this method, and Parajuli et al. obtained a LOD of ~4 mg mL^{-1} TATP [95]. Additionally, Qi et al. used ruthenium-doped silicon nanoparticles for TNT detection, through ECL quenching caused by resonant energy transfer from excited nanoparticles to a TNT–amine complex [98].

Another process for chemiluminescent-based explosives detection is upconversion luminescence. Ma et al. used nanocrystals of $NaYF_4:Yb^{3+}/Er^{3+}$ coated with amine functional groups to bind to TNT. Upon TNT binding, the fluorescence was quenched. The fluorescence quenching was found to be selective for TNT (LOD: 9.7 ng mL^{-1}) over DNT, nitrobenzene, and 2,4,6-trinitrophenol [99]. Tu et al. investigated SPR-enhanced upconversion luminescence for TNT; fluorescence increased upon addition of TNT [100].

Raman

Raman spectroscopy is one of the most heavily used and actively studied methods of explosives detection because of its powerful identification capabilities and very high selectivity, as described in recent reviews [101–103]. The molecular vibrational spectrum that Raman measures has very high information content (large number of sharp spectral features) that is distinct for different molecular structures. These variations in spectra enable the definitive identification of explosives, chemicals, and other nonmetallic materials. Raman scattering is a very inefficient process, with ~10^{-7} of incoming photons being inelastically scattered, leaving the molecule

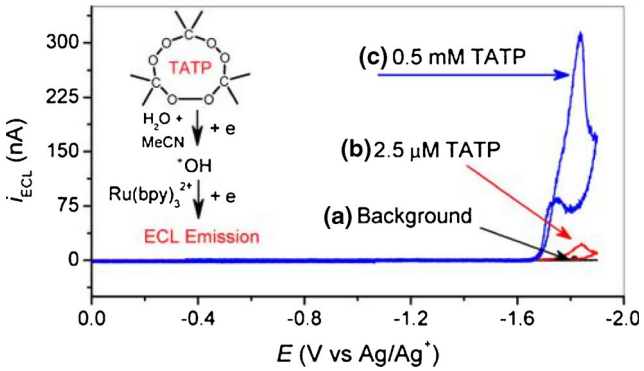

Fig. 4 Sensitive detection of TATP using electrogenerated chemiluminescence at a glassy-carbon electrode in water–acetonitrile solvent mixture. Reprinted with permission from Ref. 95. ©2010 American Chemical Society

vibrationally excited while reducing the energy of the light. Raman measurements require laser excitation, efficient collection of the scattered light, rejection of the excitation light, spectral dispersion, and detection. Several manufacturers now offer commercially available handheld Raman spectrometers that are portable, easy to use, and come equipped with extensive libraries that can identify unknown chemicals at down to μg quantities on the basis of their spectrum. The main limitation of Raman identification is the interference from fluorescence.

If the excitation light is resonantly absorbed to produce electronic excitations, either of the sample or of impurities, fluorescence emission with quantum yields often at the level of $>10^{-2}$ can swamp the Raman signal with broadband light that cannot be used for identification. Different Nd:YAG harmonics (266, 355, and 532 nm) have been compared for optimizing Raman versus fluorescence signals for explosives detection [104]. Deep-ultraviolet (DUV) resonant excitation increases the Raman cross section significantly, and can be performed at such short wavelengths that the interfering fluorescence occurs at wavelengths outside the range of the Raman spectrum [105–109]. DUV excitation is strongly absorbed and thus only probes the surface of materials, so there is a tradeoff between the higher cross section of the DUV excitation and the larger number of molecules excited with visible excitation [101]. Because UV light is absorbed in the eye before focusing on the retina, UV pulsed lasers have been demonstrated as potential explosive-detection techniques operating under eye-safe conditions, an important consideration for stand-off measurements [110–112]. Other potential solutions to the fluorescence competition are moving to longer-wavelength excitation or using sub-nanosecond time gates [113], because Raman is emitted only during the excitation pulse and fluorescence typically occurs over several nanoseconds. Alternatively, shifted excitation difference methods (taking the difference of two Raman spectra obtained with slightly shifted excitation wavelengths) can be used to remove fluorescence interference [114]. The Raman features shift with excitation wavelength, but the broad fluorescence does not. In the deep UV, Yellampalle et al. have adapted a similar scheme with the additional advantage that resonance Raman features also depend on the wavelength, resulting in substantial improvements to selectivity and reduction in false positives [115–117].

Raman at stand-off distances is typically performed with nanosecond pulsed laser excitation, collection of signal through a telescope, and gated detection with an intensified charge-coupled-device camera. These are essentially the same instrumental requirements as those of LIBS, and both are often used together [118–121]. Very good signal-to-noise has been obtained for bulk explosive materials (tens of gram quantities) in single-shot [122] and multiple-pulse [123] spectra measured beyond 100 m in daylight conditions, and at 470 m for multiple-pulse measurement (1–10 s) during heavy rainfall [124, 125].

Raman imaging can be performed in several ways, often combined with stand-off detection. A fiber array can transform the image into a linear stripe along the spectrometer slit, which enables hyperspectral image reconstruction in software [79]. The spectrometer can be replaced with a scanning liquid crystal filter [124, 126] or Fabry–Perot interferometer [112] to enable two-dimensional imaging with spectra acquired over many pulses. Alternatively, point detection can be simply scanned to construct an image [127].

Raman spectra can be measured through opaque and colored plastic containers. Spatially offset Raman spectroscopy (SORS) excites one spot on a sample and looks for multiply scattered photons collected from a spatially offset location. Photons initially from deeper in the sample have a higher probability of multiple scattering, and the ratio of signal from deep within the sample to surface excitations increases with spatial offset [128]. Time-resolved Raman spectroscopy (TRRS) uses time gating to separate surface scattered photons from those initiated deep within the sample (Fig. 5) [129]. Nitromethane inside an opaque high-density polyethylene container was detected at 15 m with SORS and TRRS, revealing good separation of signal from the container and the contents [128]. If the containers are at least partially transparent, normal stand-off Raman can be performed without any alterations [121].

Coherent Raman

Coherent Raman methods enable excitation of Raman signatures at levels that can be 10^4 times stronger than spontaneous Raman, at the expense of more complicated laser excitation sources [130, 131]. Coherent anti-Stokes Raman spectroscopy (CARS) using pulse shaping of a femtosecond supercontinuum was used for spectral identification and scanned imaging of DNT and other chemicals [132]. Femtosecond CARS with

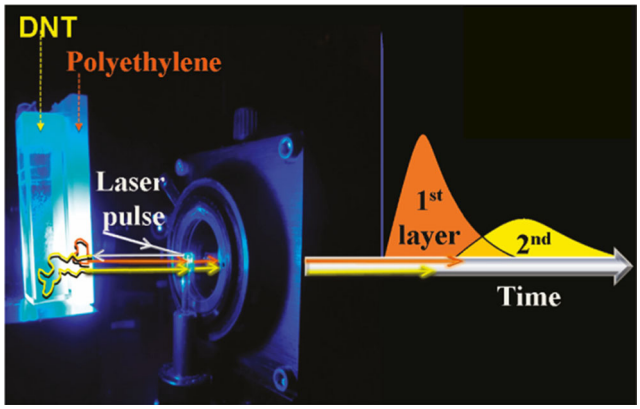

Fig. 5 Schematic of the time-resolved Raman-spectroscopy method using time gating to separate the container-wall spectra from the spectra of the material inside, enabling detection of concealed explosives inside containers. Reprinted with permission from Ref. 129. ©2011 American Chemical Society

pulse shaping for selective excitation of desired features in explosives has also been achieved [133–135]. Femtosecond stimulated Raman scattering using a pulse shaper to achieve spectral resolution (no spectrometer needed) enabled raster-scanned vibrational imaging for explosive identification to 10 m [136]. Nanosecond CARS has also achieved explosive detection and identification [131]. Coherent Raman emits signals only in the forward direction, but for solids the signal collected is light scattered in the backwards direction. An interesting possibility for detection of gases is optically pumping air so that it lases back at the excitation source, although this has not yet been developed into a practical sensing method [137].

SERS

Surface-enhanced Raman scattering (SERS) has been widely investigated as a means to exploit Raman spectroscopy for detection and identification of trace explosives [103, 138, 139] at quantities down to the monolayer level. Details of the SERS method, including plasmonic engineering for ultra-trace analysis, were reviewed by Baker and Moore [140]. One of the attractions of SERS is the ability to tune the enhancement properties by changing the size and shape of the metal nanostructure. The selectivity of SERS can also be tuned by first adsorbing molecules with different functional groups to the metal surfaces. SERS-active substrates come in many forms. Frequently, they are silver or gold nanoparticles on a dielectric substrate. Additionally, laser ablation of copper [141], silver [142], or gold [143] in solution forms a colloidal, SERS-active solution, and has been used to detect ANTA, FOX-7, and TNT.

Recently, much research has focused on the practical aspects of using SERS as an explosives detection method, including using inexpensive COTS products. Several researchers have investigated the use of Klarite™ (Renishaw Diagnostics) as a SERS substrate for explosives detection. Klarite™ consists of a regular array of gold inverted pyramid wells and has been revealed to be a suitable substrate to detect RDX [144, 145], PETN [145, 146], and TNT [145–149]. Raza et al. [150] developed an alternative inexpensive SERS test strip, consisting of silver nanoparticles grown on filter paper modified with agarose film. The test strips successfully detected TNT.

As in conventional Raman spectroscopy, the molecular SERS fingerprint can be obscured by contaminants, which is a practical consideration for the use of SERS in an explosives detection device. Researchers were able to detect 0.15 mg L^{-1} RDX in contaminated groundwater using gold nanoparticles [151], and 2 pmol L^{-1} TNT in contaminated soil using a complex hybrid microsphere composed of a poly(styrene- *co*-acrylic acid) core and magnetite shell, covered in gold nanospheres and lignin to increase the selectivity for TNT. [152]. Other research on this subject has focused on the effect of ions commonly found in groundwater and of pH on the efficacy of SERS to detect TNT and NTO [153, 154].

The spectral signatures of mixtures of materials can be difficult to separate and successfully identify using SERS. One potential solution is to use chromatography to separate components and then perform SERS on the individual constituents, as reported by Zachhuber et al. [155], who used microliquid chromatography to separate two isomers of DNT: 2,4-DNT and 2,6-DNT. Likewise, Talian et al. [156] developed silicon-based nanostructured surfaces coated with silver and gold, prepared in a microfluidic channel. They successfully separated and characterized DNB and 2,4-DNT. Jamil et al. [143] used a colloidal solution of gold nanoparticles with cysteamine in solution to increase selectivity. The cysteamine and TNT formed a Meisenheimer complex, which was then spontaneously assembled onto the gold nanoparticles and could be detected by SERS. Cysteamine was found to form the complex preferentially with TNT over DNT and picric acid.

SERS can be combined with other technologies to maximize the detection and selectivity for identification of explosives. Buettner et al. [148] combined SERS with surface-enhanced IR absorption (SEIRA) to differentiate TNT from musk ketone and musk xylene, which have similar chemical structures to TNT but are found in lotions and fragrances. They developed a plasmonic substrate comprising gold-coated silicon nanopillars that enhanced both Raman and IR. Holtoff et al. [149] integrated MIPS (molecularly imprinted polymers) with SERS, layering a TNT-imprinted xerogel over gold nanoprisms; however, the material was only sensitive to nitroaromatics.

Cavity ringdown spectroscopy

Cavity ringdown spectroscopy (CRDS) is a powerful, highly sensitive absorption-spectroscopy technique for detecting gas-phase molecules. In this technique a short laser pulse is injected into a resonant cavity with highly reflective mirrors.

As the laser pulse is reflected back and forth between the mirrors the absorbance of the molecules of interest, within the cavity, is determined by the exponential decay of the intensity of the light over time. In many cases, this method uses an optical path length many times the sample path length and measurement of the material concentration is immune to laser pulse intensity fluctuations. Spicer, Wojtas, and Caygill have recently written reviews which cover CRDS [157–159].

Many conventional explosives have very low vapor pressure, making atmospheric room temperature CRDS measurements of explosives challenging. Fortunately, NO_2 gas has a strong absorption in the UV from 400–450 nm and NO and N_2O absorb in the IR (5.26 μm and 4.55 μm, respectively). Gas concentrators [158] and catalytic reactions with platinum (IV) oxide hydrate [160] have been used to detect NO_2 down to the parts-per-billion by volume (ppbv) level. Specifically, catalytic thermal dissociation using platinum oxide hydrate on TNT, 2,4-DNT, and 1,3-DNB to produce NO_2 achieved detection at the 0.5 ppbv level using UV-CRDS without sample preconcentration after only 1 s data acquisition [160]. Wojtas reported practical application of the preconcentration technique, detecting NO_2 at a LOD of 10–100 ppbv from AN and NG in a Polish mine facility [161].

In 2010 Snels revealed that IR-CRDS (1.6–1.7 μm) did not have the sensitivity to detect explosive vapors at room temperature, but successfully detected 75 ng solid DNT and TNT when flash heated within the optical cavity [162]. Such detection limits potentially enable detection of fingerprint amounts of explosives (0.1 μg–1 mg in the first-generation print) with CRDS [162]. A free-flowing liquid wire jet soap film containing picric acid placed within the ringdown cavity at the Brewster's angle enabled detection of <17 fmol picric acid by use of a 355 nm UV-CRDS system [163].

Notable advancements have been recently made by Harb et al. [73, 164]. In 2012 they used extended Kalman filter methods or real-time data processing using a frequency-domain-analysis technique, instead of the typical Levenberg–Marquardt method, to obtain real-time detection of the vapor from a small piece of solid TNT in a CRDS cell [164]. The real-time absorption measurements were obtained while rapidly (0.2–7 s) scanning the infrared quantum cascade laser (QCL) from 1580–1700 cm^{-1}. More recently, pulsed quantum cascade systems operating in the range 1200–1320 and 1316–1613 cm^{-1} were used to measure headspace gases at ppm levels of NM and NG in less than 4 s. During the 4 s, >150,000 spectral data points were obtained and analyzed using the frequency-domain-analysis approach while scanning the QCL. This novel analysis technique enabled atmospheric-pressure and temperature measurements of NM at the ppbv level. Headspace measurements of acetone, a possible TATP impurity, were made with the sample up to a few meters away from the CRD cell input port. Future work will enable more than two lasers to be resonant in the cavity simultaneously, enabling a very large spectral bandwidth to be covered in a small amount of time [73].

Laser-induced breakdown spectroscopy

To date, most laser-induced breakdown spectroscopy (LIBS) work has been performed on conventional explosives from trace (fingerprints; μg to mg quantities) to bulk (gram) quantities [165]. Intense short-duration (femtosecond (fs) to nanosecond (ns)) laser pulses at stand-off or near-field distances are used to ablate a sample and sometimes substrate, to generate an evolving plasma. Emission from a mixture of molecules, atoms, and ions in a variety of rapidly evolving excited states is collected, and chemometrics/analysis of the C, H, O, N, Cl, and CN components is performed. Reviews within the past five years cover the different techniques [101, 165–170]. Recent work has revealed the effects of substrate and interferent dependence [171] on analyte classification and how selective sampling can enable surface sensitivity [172–176]. Effects caused by wind [177], thermal radiation [166, 178, 179], and different atmospheres [179–181] were also investigated.

Signal enhancement through dual-pulse LIBS increased analyte signal by up to an order of magnitude, but was found to be dependent on the substrate and element investigated [165]. Using a CO_2 laser as the second pulse efficiently reheats the plasma plume through an inverse Bremsstrahlung absorption process, without increasing the quantity of ablated mass [166, 182]. More recently a geometry-dependent, single-beam-splitting LIBS approach obtained signal enhancement (~5×) resulting from the angle and energy of the second beam and not the timing [183]. Remote filamentation-induced breakdown spectroscopy (R-FIBS) uses ultrashort fs lasers to induce a filament in the atmosphere over distances of up to a kilometer, with no need for focusing optics [168]. In general, the ultrashort timescale of fs-LIBS enables ablation of the sample material before energy has time to transfer into the substrate, enabling detection of smaller amounts of material. Elemental emission is fluence dependent, so more energy results in more signal [184] and the lower-temperature plasmas observed in fs-LIBS result in less fragmentation of the explosive molecules and subsequently larger molecular fragment emissions [185]. Time-resolved fs-LIBS experiments on RDX, TNT, and NTO under different atmospheres reveal that CN emission is from a secondary reaction from the surrounding nitrogen environment within 150 ns [181].

Some improvised explosives and their precursors have been investigated using LIBS excited at 1064 nm [186]. An important advance in observing molecular fragment emissions in the mid-wave IR and long-wave IR from 4–12 μm was achieved by Yang et al. [187]. High-energy (>10 mJ) fs-LIBS (<750 fs) enabled preservation of the 420 nm NO_x signature from KNO_2 and $NaNO_3$ [185]. Weathering effects

on chloratite (a mixture of $NaClO_3$, $KClO_3$, sulfur, and sugar) fingerprints (Fig. 6) revealed that a good signal was obtainable for only two weeks [173].

Much effort has been made in the chemometrics/analysis of LIBS emission spectra to enhance classification models and decrease the number of false positives [188, 189]. Linear analysis was found to be insufficient, necessitating multivariate analysis [190]. Partial-least-squares discriminant analysis [175, 178, 191] and machine-learning classifiers with supervised learning methods [172, 189, 192] are two of the more common techniques. Combining LIBS with Raman spectroscopy has increased the ability to identify unknown materials at stand-off distances through sensor–data fusion (Fig. 7 shows an example) [119, 193–196]. As high-energy lasers become more portable, the suitability of LIBS for use in the field is improving [168, 184, 197]. Handheld low-power (<1 mW) 1064 nm LIBS devices are currently commercially available for metal analysis, indicating that applications to explosives detection are not far behind [198, 199].

Photoacoustic spectroscopy

In typical laser photoacoustic spectroscopy (PAS), alternating electromagnetic radiation (pulsed alternating with chopped) is absorbed by a sample and converted into heat by a non-radiative de-excitation process. Ambient air absorbs the heat, and the rapid sample heating and cooling caused by the alternating chopped and pulsed light causes a pressure fluctuation or photoacoustic wave that can be monitored using a microphone or laser vibrometer [200]. Use of a cavity cell containing a gas or solid material and enhanced microphones has obtained better than ppbv detection sensitivity for trace gas analysis of non-explosives [201]. To enhance the photoacoustic signal to a part per trillion (pptv) detection level, piezoelectric transducers [202, 203], as simple as a quartz resonator in the form of a tuning fork, can be used; this method is called quartz-enhanced laser photoacoustic spectroscopy (QE-PAS) [203]. PAS signal strength is proportional to laser pulse energy. In stand-off PAS, as the acoustic wave propagates, the pressure amplitude signal strength decays with a 1/r dependence [202].

Photoacoustic spectroscopy is selective (characteristic rotational and vibrational absorption) and sensitive (~1 ng TNT [204]), and can be used without sample preparation. It is also advantageous because it is not sensitive to light scattering caused by the substrate, but only to absorption of optical radiation [204]. However, care must be taken to ensure there are not interferences from other substances including atmospheric gases [205], other explosives, and background noise [206]. Ideally the background and/or sample surface should be transparent to the effects of the excitation laser, but in practical application this is problematic. The sensitivity or selectivity of PAS can be enhanced by combining it with other detection techniques, for example resonant microcantilevers or UV spectroscopy. The works of Dongkyu and Van Neste are good examples of combined techniques [207, 208]. A portable off-the-shelf PAS device uses UV light to vaporize and dissociate materials such as explosives, which then emit ultrasonic photoacoustic signals [209].

Recent advancements with quantum cascade lasers (QCL) have led to enhanced photoacoustic techniques whereby the sample surface is exposed to tunable laser radiation within the material's characteristic absorption band. As the laser wavelength is scanned the photoacoustic response is measured using a microphone or QE-PAS, and photoacoustic spectra corresponding to the rotational–vibrational energy absorption specific to the chemical species are obtained. In 2010, QE-PAS was successfully used in a 20 m stand-off configuration with a 100 mW QCL (9.25–9.80 μm) to detect RDX at a surface concentration of ~100 ng cm^{-2} [210]. The work of Sharma et al. revealed that stand-off distance was dependent on the background substrate material. DNT and PETN on diffused Al, scanned over 1160–1400 cm^{-1} and 880–915cm^{-1}, had a 5 μg cm^{-2} sensitivity with 12 m range, whereas a wood surface required 50 μg cm^{-2} to yield only a 6 m range [211]. Short stand-off detection (8 inches) of bulk TNT (1 mg mm^{-2}) was obtained using an ultrasensitive microphone, and increased to 2.5 m using a 0.6 m diameter parabolic sound reflector [202, 206]. The C–O stretch, centered near 8.3 μm, of the homemade explosive TATP was detected in the gas phase in the near field using QE-PAS [205, 212]. Multivariate analysis has also been used in combination with IR (9–11 μm, 30–500 mW) scanning PAS in a cavity cell configuration to identify less than 100 μg DNT, TNT, Tetryl, RDX, HMX, PETN, and TATP [213].

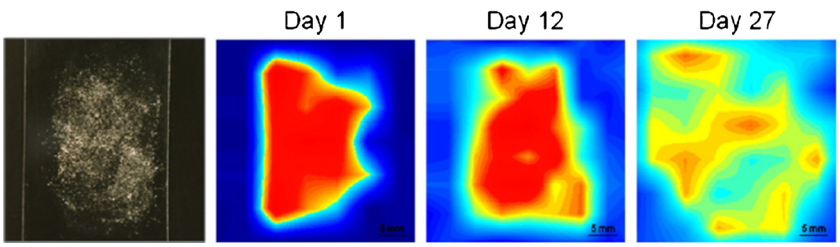

Fig. 6 Linear LIBS scanning of weathered chloratite fingerprints on Al surface at 31 m stand-off. Emission from Na line at 589.2 nm shown as a function of increasing age after deposition. Reprinted with permission from Ref. 173. ©2013 Elsevier

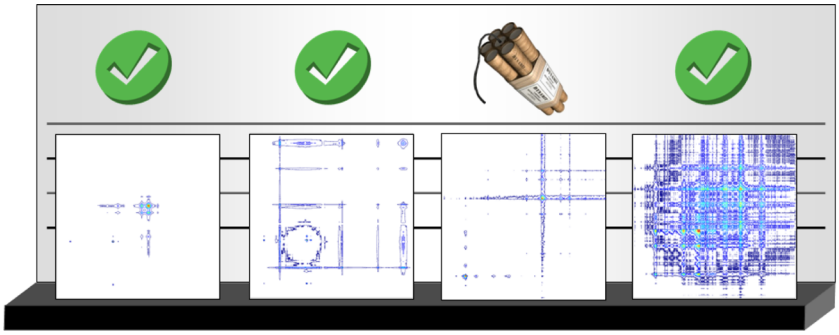

Fig. 7 Illustration of Raman–LIBS spectral output fusion. The process uses a mathematical treatment to produce a two-dimensional image of target analytes and matrix and/or interference materials by assembling the Raman and LIBS spectra and using simple correlation coefficient values from the two-dimensional images and those achieved using Raman and LIBS spectra separately. Reprinted with permission from Ref. 195. © 2011 American Chemical Society

Outlook

The expanding number, quality, and breadth of explosives detection methods are encouraging the development of ever more capable instruments, for both laboratory and field use. Instrumentation for X-ray diffraction methods is being rapidly advanced, so that the identification advantages of X-ray diffraction over X-ray imaging can be realized in screening applications. Terahertz imaging with spectral resolution seems to be on the brink of application for enhanced personnel screening applications with the ability to identify contraband materials, although challenges related to spectral feature modification caused by texture or covering materials must still be resolved. Both active and passive infrared spectral imaging methods are improving their detection limits and their identification abilities. However, methods must improve their abilities in backscattering or emission geometries, which can cause peaks to look absorptive, dispersive, or intermediate between the two as a result of particle size, shape, and environment. We look forward to important developments where chemiluminescence technologies are embodied into swipe or glove-type sampling methods to analyze suspect areas or investigate individuals or objects in close to real time. Although Raman seems to be one of the most mature explosives detection methods, substantial improvements are still possible, including new hardware for Raman imaging, further reduction in fluorescence interference, as in SORS or TRRS, via novel laser sources, wavelength modulation, or new detectors, and combinations of Raman with other technology (beyond ATR-FTIR or LIBS, which are currently actively pursued). Similarly, hybridization of methods, for example SERS with SEIRA or MIPS, and advances in data-fusion computational tools will lead to improved ROC curves and areas of application. Large-area screening for trace gases indicative of contraband materials is quickly being realized, especially using new cavity ringdown spectroscopic methods and other long-path absorption tools. Data-fusion methods are improving the probability of detection and identification from ever-smaller samples and ever more complicated explosive materials, including the increasingly prevalent homemade explosives. Nevertheless, methods to fuse data or information from more disparate and larger numbers of methods to achieve greater certainty of detection or increased discrimination between threat and non-threat are needed.

Acknowledgements Los Alamos National Laboratory is operated by Los Alamos National Security, LLC, for the National Nuclear Security Administration of the U.S. Department of Energy under Contract No. DE-AC52-06NA25396. The authors gratefully acknowledge the support of this study by Eric Sanders.

Conflict of interest The authors declare that they have no potential conflict of interest.

References

1. Brown KE, Greenfield MT, McGrane, SD, Moore, DS (2015) Advances in explosives analysis - part I: animal, chemical, ion, and mechanical methods. Anal Bioanal Chem. doi:10.1007/s00216-015-9040-4
2. Zhong Y, Li MQ, Sun B, Wang J, Zhang F, Yu DY, Zhang Y, Liu JH (2012) Non-invasive investigation of liquid materials using energy dispersive X-ray scattering. Measurement 45(6):1540–1546. doi:10.1016/j.measurement.2012.02.024
3. Wells K, Bradley DA (2012) A review of X-ray explosives detection techniques for checked baggage. Appl Radiat Isot 70(8):1729–1746. doi:10.1016/j.apradiso.2012.01.011
4. Greenberg JA, Krishnamurthy K, Brady D (2013) Snapshot molecular imaging using coded energy-sensitive detection. Opt Express 21(21):25480–25491. doi:10.1364/oe.21.025480
5. Harding G, Fleckenstein H, Kosciesza D, Olesinski S, Strecker H, Theedt T, Zienert G (2012) X-ray diffraction imaging with the multiple inverse Fan beam topology: principles, performance and potential for security screening. Appl Radiat Isot 70(7):1228–1237. doi:10.1016/j.apradiso.2011.12.015
6. O'Flynn D, Reid CB, Christodoulou C, Wilson MD, Veale MC, Seller P, Hills D, Desai H, Wong B, Speller R (2013) Explosive detection using pixellated X-ray diffraction (PixD). Journal of Instrumentation 8. doi:10.1088/1748-0221/8/03/p03007
7. Crespy C, Duvauchelle P, Kaftandjian V, Soulez F, Ponard P (2010) Energy dispersive X-ray diffraction to identify explosive substances: Spectra analysis procedure optimization. Nuclear

Instrum Methods Phys Res Sect Accelerators Spectrometers Detectors Assoc Equipment 623(3):1050–1060. doi:10.1016/j.nima.2010.08.023
8. Greenberg JA, Brady DJ (2014) Structured illumination for compressive x-ray diffraction tomography. Computational Imaging Xii 9020. doi:10.1117/12.2048264
9. Evans P, Rogers K, Dicken A, Godber S, Prokopiou D (2014) X-ray diffraction tomography employing an annular beam. Opt Express 22(10):11930–11944. doi:10.1364/oe.22.011930
10. Prokopiou D, Rogers K, Evans P, Godber S, Dicken A (2013) Discrimination of liquids by a focal construct X-ray diffraction geometry. Appl Radiat Isot 77:160–165. doi:10.1016/j.apradiso.2013.03.051
11. Sun B, Li MQ, Zhang F, Zhong Y, Kang NS, Lu W, Liu JH (2010) The performance of a fast testing system for illicit materials detection based on energy-dispersive X-ray diffraction technique. Microchem J 95(2):293–297. doi:10.1016/j.microc.2009.12.018
12. Dicken A, Rogers K, Evans P, Rogers J, Chan JW (2010) The separation of X-ray diffraction patterns for threat detection. Appl Radiat Isot 68(3):439–443. doi:10.1016/j.apradiso.2009.11.072
13. Vila FD, Jach T, Elam WT, Rehr JJ, Denlinger JD (2011) X-ray emission spectroscopy of nitrogen-rich compounds. J Phys Chem A 115(15):3243–3250. doi:10.1021/jp108539v
14. McLeod JA, Kurmaev EZ, Sushko PV, Boyko TD, Levitsky IA, Moewes A (2012) Selective response of mesoporous silicon to adsorbants with nitro groups. Chem Eur J 18(10):2912–2922. doi:10.1002/chem.201102084
15. Goldberg IG, Vila FD, Jach T (2012) Surface effects on the crystallization of cyclo-1,3,5-trimethylene-2,4,6-trinitramine (RDX) and the consequences for its N K X-ray emission spectrum. J Phys Chem A 116(40):9897–9899. doi:10.1021/jp306978x
16. Whetstone ZD, Kearfott KJ (2014) A review of conventional explosives detection using active neutron interrogation. J Radioanal Nucl Chem 301(3):629–639. doi:10.1007/s10967-014-3260-5
17. McFee JE, Faust AA, Pastor KA (2013) Photoneutron spectroscopy using monoenergetic gamma rays for bulk explosives detection. Nucl Inst Methods Phys Res Section Accelerators Spectrometers Detectors Assoc Equip 704:131–139. doi:10.1016/j.nima.2012.12.053
18. Yigang Y, Jianbo Y, Yuanjing L (2013) Fusion of X-ray imaging and photoneutron induced gamma analysis for contrabands detection. IEEE Trans Nucl Sci 60(2):1134–1139. doi:10.1109/tns.2013.2248095
19. Skoulakis A, Androulakis GC, Clark EL, Hassan SM, Lee P, Chatzakis J, Bakarezos M, Dimitriou V, Petridis C, Papadogiannis NA, Tatarakis M (2014) A portable pulsed neutron generator. Int J Mod Phys: Conf Ser 27:1460127. doi:10.1142/s2010194514601276
20. McFee JE, Faust AA, Andrews HR, Clifford ETH, Mosquera CM (2013) Performance of an improved thermal neutron activation detector for buried bulk explosives. Nucl Instrum Methods Phys Res Section a-Accelerators Spectrometers Detectors Assoc Equip 712:93–101. doi:10.1016/j.nima.2013.02.008
21. Kettler J, Mauerhofer E, Steinbusch M (2013) Detection of unexploded ordnance by PGNAA based borehole-logging. J Radioanal Nucl Chem 295(3):2071–2075. doi:10.1007/s10967-012-2215-y
22. Batyaev VF, Belichenko SG, Bestaev RR, Gavryuchenkov AV (2014) Ultimate levels of explosives detection via tagged neutrons. Int J Mod Phys: Conf Ser 27:1460131. doi:10.1142/s2010194514601318
23. Trofimov VA, Varentsova SA, Chen J (2010) Identification of explosive using the spectrum dynamics of reflected THz and GHz radiation. Millimetre Wave and Terahertz Sensors and Technology Iii 7837. doi:10.1117/12.864873
24. Trzcinski T, Palka N, Szustakowski M (2011) THz spectroscopy of explosive-related simulants and oxidizers. Bull Polish Acad Sci Techn Sci 59(4):445–447. doi:10.2478/v10175-011-0056-4
25. Walczakowski M, Palka N, Szustakowski M, Czerwinski A, Sypek M (2013) Detection of the THz waves from the 5-m distance. Millimetre Wave and Terahertz Sensors and Technology Vi 8900. doi:10.1117/12.2028852
26. Maestrojuan I, Palacios I, Etayo D, Iriarte JC, Teniente J, Ederra I, Gonzalo R (2011) Explosives Characterization in Terahertz Range. Millimetre Wave and Terahertz Sensors and Technology Iv 8188. doi:10.1117/12.898152
27. Etayo D, Maestrojuan I, Teniente J, Ederra I, Gonzalo R (2013) Experimental explosive characterization for counterterrorist investigation. J Infrared Millimeter Terahertz Waves 34(7–8):468–479. doi:10.1007/s10762-013-9988-0
28. Sleiman JB, El Haddad J, Perraud JB, Bassel L, Bousquet B, Palka N, Mounaix P (2014) Qualitative and quantitative analysis of explosives by terahertz time-domain spectroscopy: Application to imaging. 2014 39th International Conference on Infrared, Millimeter, and Terahertz waves. doi:10.1109/IRMMW-THz.2014.6956226
29. Barber J, Weatherall JC, Smith BT, Duffy S, Goettler SJ, Krauss RA (2010) Millimeter wave measurements of explosives and simulants. Proc of SPIE Passive Millimeter-Wave Imaging Technology XIII 7670:76700E-76700E-76707
30. van Rheenen AD, Haakestad MW (2011) Detection and identification of explosives hidden under barrier materials - what are the THz-technology challenges? Detection and Sensing of Mines, Explosive Objects, and Obscured Targets Xvi 8017. doi:10.1117/12.886108
31. Trofimov VA, Varentsova SA, Szustakowski M, Palka N (2012) Efficiency of the detection and identification of ceramic explosive using the reflected THz signal. Terahertz Physics, Devices, and Systems Vi: Advanced Applications in Industry and Defense 8363. doi:10.1117/12.919750
32. Choi J, Ryu SY, Kwon WS, Kim K-S, Kim S (2013) Compound explosives detection and component analysis via terahertz time-domain spectroscopy. J Opt Soc Korea 17(5):454–460. doi:10.3807/josk.2013.17.5.454
33. Gavenda T, Kresalek V (2013) Terahertz time-domain spectroscopy for distinguishing different kinds of gunpowder. Millimetre Wave and Terahertz Sensors and Technology Vi 8900. doi:10.1117/12.2034126
34. Witko EM, Buchanan WD, Korter TM (2011) Terahertz spectroscopy and solid-state density functional theory simulations of the improvised explosive oxidizers potassium nitrate and ammonium nitrate. J Phys Chem A 115(44):12410–12418. doi:10.1021/jp2075429
35. Khachatrian A, Melinger JS, Qadri SB (2012) Waveguide terahertz time-domain spectroscopy of ammonium nitrate polycrystalline films. Journal of Applied Physics 111 (9):-. doi:doi:http://dx.doi.org/10.1063/1.4709385
36. Witko EM, Korter TM (2012) Terahertz spectroscopy of the explosive taggant 2,3-dimethyl-2,3-dinitrobutane. J Phys Chem A 116(25):6879–6884. doi:10.1021/jp302487t
37. Kemp MC (2011) Explosives detection by terahertz spectroscopy-a bridge Too Far? Ieee Trans Terahertz Sci Technol 1(1):282–292. doi:10.1109/tthz.2011.2159647
38. Palka N (2013) Identification of concealed materials, including explosives, by terahertz reflection spectroscopy. Opt Eng 53(3):031202–031202. doi:10.1117/1.OE.53.3.031202
39. Palka N (2013) Detection of covered materials in the TDS-THz setup. Terahertz Physics, Devices, and Systems Vii: Advanced Applications in Industry and Defense 8716. doi:10.1117/12.2015373

40. Trofimov VA, Peskov NV, Kirillov DA (2012) Efficiency of using correlation function for estimation of probability of substance detection on the base of THz spectral dynamics. Terahertz Emitters, Receivers, and Applications Iii 8496. doi:10.1117/12.927441
41. Trofimov VA, Trofimov VV, Deng C, Zhao Y-m, Zhang C-l, Zhang X (2011) Possible way for increasing the quality of imaging from THz passive device. Optics and Photonics for Counterterrorism and Crime Fighting Vii Optical Materials in Defence Systems Technology Viii and Quantum-Physics-Based Information Security 8189. doi:10.1117/12.897900
42. Trofimov VA, Trofimov VV, Kuchik IE (2014) Temperature resolution enhancing of commercially available THz passive cameras due to computer processing of images. Passive and Active Millimeter-Wave Imaging Xvii 9078. doi:10.1117/12.2049413
43. Zhao R, Zhao Y-m, Deng C, Zhang C-l, Li Y (2014) Target Recognition in Passive Terahertz Image of Human Body. Infrared, Millimeter-Wave, and Terahertz Technologies Iii 9275. doi:10.1117/12.2073957
44. Henry SC, Schecklman S, Kniffin GP, Zurk LM, Chen A (2010) Measurement and Modeling of Rough Surface Effects on Terahertz Spectroscopy. Terahertz Technology and Applications Iii 7601. doi:10.1117/12.841054
45. Zurk LM, Henry SC, Schecklman S, Duncan DD (2010) Physics-based processing for terahertz reflection spectroscopy and imaging. Infrared, Millimeter Wave, and Terahertz Technologies 7854. doi:10.1117/12.870664
46. Schecklman S, Zurk LM, Henry S, Kniffin GP (2011) Terahertz material detection from diffuse surface scattering. Journal of Applied Physics 109 (9). doi:10.1063/1.3561806
47. Henry SC, Kniffin GP, Zurk LM (2012) 3-D broadband terahertz synthetic aperture imaging. 2012 37th International Conference on Infrared, Millimeter, and Terahertz Waves. doi:10.1109/IRMMW-THz.2012.6380366
48. Henry SC, Zurk LM, Schecklman S (2013) Terahertz spectral imaging using correlation processing. Ieee Trans Terahertz Sci Technol 3(4):486–493. doi:10.1109/tthz.2013.2261065
49. Startsev MA, Elezzabi AY (2013) Terahertz frequency continuous-wave spectroscopy and imaging of explosive substances. ISRN Optics 2013:8. doi:10.1155/2013/419507
50. Palka N, Szustakowski M, Kowalski M, Trzcinski T, Ryniec R, Piszczek M, Ciurapinski W, Zyczkowski M, Zagrajek P, Wrobel J (2012) THz spectroscopy and imaging in security applications. 2012 19th International Conference on Microwaves, Radar & Wireless Communications. doi:10.1109/mikon.2012.6233513
51. Carriere JTA, Havermeyer F, Heyler RA (2013) THz-Raman Spectroscopy for Explosives, Chemical and Biological Detection. Chemical, Biological, Radiological, Nuclear, and Explosives (Cbrne) Sensing Xiv 8710. doi:10.1117/12.2018095
52. Heyler RA, Carriere JTA, Havermeyer F (2013) THz-Raman - Accessing molecular structure with Raman spectroscopy for enhanced chemical identification, analysis and monitoring. Next-Generation Spectroscopic Technologies Vi 8726. doi:10.1117/12.2018136
53. Carriere JTA, Havermeyer F, Heyler RA (2014) Improving Sensitivity and Source Attribution of Homemade Explosives with Low Frequency/THz-Raman (R) Spectroscopy. Chemical, Biological, Radiological, Nuclear, and Explosives (Cbrne) Sensing Xv 9073. doi:10.1117/12.2053461
54. Lu W, Argyros A (2014) Terahertz spectroscopy and imaging with flexible tube-lattice fiber probe. J Lightwave Technol 32(23): 4019–4025. doi:10.1109/jlt.2014.2361145
55. Perov AN, Zaytsev KI, Fokina IN, Karasik VE, Yakovlev EV, Yurchenko SO, Iop (2014) BWO based THz imaging system. 2nd Russia-Japan-USA Symposium on the Fundamental and Applied Problems of Terahertz Devices and Technologies (Rjus Teratech - 2013) 486. doi:10.1088/1742-6596/486/1/012027
56. Simoens F, Arnaud A, Castelein P, Goudon V, Imperinetti P, Dera JL, Meilhan J, Buffet JLO, Pocas S, Maillou T, Hairault L, Gellie P, Barbieri S, Sirtori C (2010) Development of uncooled antenna-coupled microbolometer arrays for explosive detection and identification. Millimetre Wave and Terahertz Sensors and Technology Iii 7837. doi:10.1117/12.865189
57. Simoens F, Meilhan J, Delplanque B, Gidon S, Lasfargues G, Dera JL, Nguyen DT, Ouvrier-Buffet JL, Pocas S, Maillou T, Cathabard O, Barbieri S (2012) Real-time imaging with THz fully-customized uncooled amorphous-silicon microbolometer focal plane arrays. Terahertz Physics, Devices, and Systems Vi: Advanced Applications in Industry and Defense 8363. doi:10.1117/12.919185
58. Bolduc M, Terroux M, Tremblay B, Marchese L, Savard E, Doucet M, Oulachgar H, Alain C, Jerominek H, Bergeron A (2011) Noise-equivalent power characterization of an uncooled microbolometer-based THz imaging camera. Terahertz Physics, Devices, and Systems V: Advance Applications in Industry and Defense 8023. doi:10.1117/12.883507
59. Castro-Suarez JR, Pacheco-Londono LC, Ortiz-Rivera W, Velez-Reyes M, Diem M, Hernandez-Rivera SP (2011) Open Path FTIR Detection of Threat Chemicals in Air and on Surfaces. Infrared Technology and Applications Xxxvii 8012. doi:10.1117/12.884436
60. Bingham AL, Lucey PG, Akagi JT, Hinrichs JL, Knobbe ET (2014) LWIR hyperspectral micro-imager for detection of trace explosive particles. Next-Generation Spectroscopic Technologies Vii 9101. doi:10.1117/12.2050824
61. Theriault J-M, Montembeault Y, Lavoie H, Bouffard F, Fortin G, Lacasse P, Vallieres A, Puckrin E, Farley V, Chamberland D, Bubner T (2011) A novel infrared hyperspectral imager for passive standoff detection of explosives and explosive precursors. Chemical, Biological, Radiological, Nuclear, and Explosives (CBRNE) Sensing XII 8018. doi:10.1117/12.884327
62. Wagner J, Ostendorf R, Grahmann J, Merten A, Hugger S, Jarvis JP, Fuchs F, Boskovic D, Schenk H (2015) Widely tuneable quantum cascade lasers for spectroscopic sensing. Quantum Sensing and Nanophotonic Devices Xii 9370. doi:10.1117/12.2082794
63. Price SR, Anderson DT, Luke RH, Stone K, Keller JM (2013) Automatic detection system for buried explosive hazards in FL-LWIR based on soft feature extraction using a bank of Gabor energy filters. Detection and Sensing of Mines, Explosive Objects, and Obscured Targets Xviii 8709. doi:10.1117/12.2014781
64. Pacheco-Londono LC, Castro-Suarez JR, Aparicio-Bolanos J, Hernandez-Rivera SP (2013) Angular Dependence of Source-Target-Detector in Active Mode Standoff Infrared Detection. Sensors, and Command, Control, Communications, and Intelligence (C3i) Technologies for Homeland Security and Homeland Defense Xii 8711. doi:10.1117/12.2016153
65. Zhang Z, Clewes RJ, Howle CR, Reid DT (2014) Active FTIR-based stand-off spectroscopy using a femtosecond optical parametric oscillator. Opt Lett 39(20):6005–6008. doi:10.1364/ol.39.006005
66. Mukherjee A, Von der Porten S, Patel CKN (2010) Standoff detection of explosive substances at distances of up to 150 m. Appl Opt 49(11):2072–2078. doi:10.1364/ao.49.002072
67. Fuchs F, Hugger S, Jarvis J, Blattmann V, Kinzer M, Yang QK, Ostendorf R, Bronner W, Driad R, Aidam R, Wagner J (2013) Infrared Hyperspectral Standoff Detection of Explosives. Chemical, Biological, Radiological, Nuclear, and Explosives (CBRNE) Sensing XIV 8710. doi:10.1117/12.2015682
68. Fuchs F, Hugger S, Kinzer M, Yang QK, Bronner W, Aidam R, Degreif K, Rademacher S, Schnuerer F, Schweikert W (2012) Standoff detection of explosives with broad band tunable external

cavity quantum cascade lasers. Quantum Sensing and Nanophotonic Devices Ix 8268. doi:10.1117/12.908119
69. Bernacki BE, Phillips MC (2010) Standoff hyperspectral imaging of explosives residues using broadly tunable external cavity quantum cascade laser illumination. Chemical, Biological, Radiological, Nuclear, and Explosives (CBRNE) Sensing Xi 7665. doi:10.1117/12.849543
70. Degreif K, Rademacher S, Dasheva P, Fuchs F, Hugger S, Schnuerer F, Schweikert W (2011) Stand-off explosive detection on surfaces using multispectral MIR-Imaging. Quantum Sensing and Nanophotonic Devices Viii 7945. doi:10.1117/12.874044
71. Suter JD, Bernacki B, Phillips MC (2012) Spectral and angular dependence of mid-infrared diffuse scattering from explosives residues for standoff detection using external cavity quantum cascade lasers. Appl Phys B-Lasers Optics 108(4):965–974. doi:10.1007/s00340-012-5134-2
72. Macleod NA, Molero F, Weidmann D (2015) Broadband standoff detection of large molecules by mid-infrared active coherent laser spectrometry. Opt Express 23(2):912–928. doi:10.1364/oe.23.000912
73. Boyson TK, Rittman DR, Spence TG, Calzada ME, Kallapur AG, Petersen IR, Kirkbride KP, Moore DS, Harb CC (2014) Pulsed quantum cascade laser based hypertemporal real-time headspace measurements. Opt Express 22(9):10519–10534. doi:10.1364/oe.22.010519
74. Patel CKN (2011) Quantum Cascade Lasers: A Game Changer for Defense and Homeland Security IR Photonics. Micro- and Nanotechnology Sensors, Systems, and Applications Iii 8031. doi:10.1117/12.885806
75. Furstenberg R, Kendziora C, Papantonakis M, Viet N, McGill RA (2014) The challenge of changing signatures in infrared stand-off detection of trace explosives. Chemical, Biological, Radiological, Nuclear, and Explosives (CBRNE) Sensing XV 9073. doi:10.1117/12.2050621
76. Deutsch ER, Haibach FG, Mazurenko A (2012) Detection and Quantification of Explosives and CWAs using a Handheld Widely-Tunable Quantum Cascade Laser. Next-Generation Spectroscopic Technologies V 8374. doi:10.1117/12.919554
77. Fernandez A, de la Ossa M, Amigo JM, Garcia-Ruiz C (2014) Detection of residues from explosive manipulation by near infrared hyperspectral imaging: A promising forensic tool. Forensic Sci Int 242:228–235. doi:10.1016/j.forsciint.2014.06.023
78. Fernandez de la Ossa MA, Garcia-Ruiz C, Amigo JM (2014) Near infrared spectral imaging for the analysis of dynamite residues on human handprints. Talanta 130:315–321. doi:10.1016/j.talanta.2014.07.026
79. Gomer NR, Gardner CW (2014) STARR: shortwave-targeted agile Raman robot for the detection and identification of emplaced explosives. Chemical, Biological, Radiological, Nuclear, and Explosives (CBRNE) Sensing XV 9073. doi:10.1117/12.2050647
80. Kumar M, Islam MN, Terry FL Jr, Freeman MJ, Chan A, Neelakandan M, Manzur T (2012) Stand-off detection of solid targets with diffuse reflection spectroscopy using a high-power mid-infrared supercontinuum source. Appl Opt 51(15):2794–2807. doi:10.1364/ao.51.002794
81. Dubroca T, Guetard G, Hummel RE (2012) Influence of spatial differential reflection parameters on 2,4,6-trinitrotoluene (TNT) absorption spectra. Chemical, Biological, Radiological, Nuclear, and Explosives (CBRNE) Sensing XIII 8358. doi:10.1117/12.918385
82. Dubroca T, Moyant K, Hummel RE (2013) Ultra-violet and visible absorption characterization of explosives by differential reflectometry. Spectrochim Acta Part A Mol Biomol Spectrosc 105:149–155. doi:10.1016/j.saa.2012.11.090
83. Dubroca T, Brown G, Hummel RE (2014) Detection of explosives by differential hyperspectral imaging. Optical Engineering 53 (2). doi:10.1117/1.oe.53.2.021112
84. Buryakov IA, Buryakov TI, Matsaev VT (2014) Optical chemical sensors for the detection of explosives and associated substances. J Anal Chem 69(7):616–631. doi:10.1134/s1061934814070041
85. Hu Z, Deibert BJ, Li J (2014) Luminescent metal-organic frameworks for chemical sensing and explosive detection. Chem Soc Rev 43(16):5815–5840. doi:10.1039/C4CS00010B
86. Xu H, Liu F, Cui Y, Chen B, Qian G (2011) A luminescent nanoscale metal-organic framework for sensing of nitroaromatic explosives. Chem Commun 47(11):3153–3155. doi:10.1039/C0CC05166G
87. Wu Z-F, Tan B, Feng M-L, Lan A-J, Huang X-Y (2014) A magnesium MOF as a sensitive fluorescence sensor for CS2 and nitroaromatic compounds. J Mater Chem A 2(18):6426–6431. doi:10.1039/C3TA15071B
88. Ma J, Lv L, Zou G, Zhang Q (2015) Fluorescent porous film modified polymer optical fiber via “click” chemistry: stable Dye dispersion and trace explosive detection. ACS Appl Mater Interfaces 7(1):241–249. doi:10.1021/am505950c
89. Sun X, Bruckner C, Nieh M-P, Lei Y (2014) A fluorescent polymer film with self-assembled three-dimensionally ordered nanopores: preparation, characterization and its application for explosives detection. J Mater Chem A 2(35):14613–14621. doi:10.1039/C4TA02554G
90. Ma H, Gao R, Yan D, Zhao J, Wei M (2013) Organic-inorganic hybrid fluorescent ultrathin films and their sensor application for nitroaromatic explosives. J Mater Chem C 1(26):4128–4137. doi:10.1039/C3TC30142G
91. Li H, Wang J, Pan Z, Cui L, Xu L, Wang R, Song Y, Jiang L (2011) Amplifying fluorescence sensing based on inverse opal photonic crystal toward trace TNT detection. J Mater Chem 21(6):1730–1735. doi:10.1039/c0jm02554b
92. Li X, Zhang Z, Tao L (2013) A novel array of chemiluminescence sensors for sensitive, rapid and high-throughput detection of explosive triacetone triperoxide at the scene. Biosens Bioelectron 47:356–360. doi:10.1016/j.bios.2013.03.002
93. Shaw A, Calhoun RL (2012) Electrogenerated Chemiluminescence with Ruthenium Trisbipyridine and TATP. In: Mantz RA, Suroviec A (eds) Physical and Analytical Electrochemistry, vol 41. ECS Transactions, vol 27. pp 49–56. doi:10.1149/1.3692523
94. Shaw A, Lindhome P, Calhoun RL (2013) Electrogenerated Chemiluminescence (ECL) Quenching of Ru(bpy)(3)(2+) by the Explosives TATP and Tetryl. J Electrochem Soc 160(10):H782–H786. doi:10.1149/2.005311jes
95. Parajuli S, Miao W (2013) Sensitive Determination of Triacetone Triperoxide Explosives Using Electrogenerated Chemiluminescence. Anal Chem 85(16):8008–8015. doi:10.1021/ac401962b
96. Donaldson DN, Barnett NW, Agg KM, Graham D, Lenehan CE, Prior C, Lim KF, Francis PS (2012) Chemiluminescence detection of 1,3,5-trinitro-1,3,5-triazacyclohexane (RDX) and related nitramine explosives. Talanta 88:743–748. doi:10.1016/j.talanta.2011.11.051
97. Ni X, Zhao Y, Song Q (2015) Electrochemical reduction and in-situ electrochemiluminescence detection of nitroaromatic compounds. Electrochim Acta 164:31–37. doi:10.1016/j.electacta.2015.02.174
98. Qi W, Xu M, Pang L, Liu Z, Zhang W, Majeed S, Xu G (2014) Electrochemiluminescence Detection of TNT by Resonance Energy Transfer through the Formation of a TNT-Amine Complex. Chem-A Eur J 20(16):4829–4835. doi:10.1002/chem.201303710

99. Ma Y, Wang L (2014) Upconversion luminescence nanosensor for TNT selective and label-free quantification in the mixture of nitroaromatic explosives. Talanta 120:100–105. doi:10.1016/j.talanta.2013.12.009
100. Tu N, Wang L (2013) Surface plasmon resonance enhanced upconversion luminescence in aqueous media for TNT selective detection. ChemCommun 49(56):6319–6321. doi:10.1039/C3CC43146K
101. Fountain AW, Christesen SD, Moon RP, Guicheteau JA, Emmons ED (2014) Recent Advances and Remaining Challenges for the Spectroscopic Detection of Explosive Threats. Appl Spectrosc 68(8):795–811. doi:10.1366/14-07560
102. Fountain AW, III, Guicheteau JA, Pearman WF, Chyba TH, Christesen SD (2010) Long Range Standoff Detection of Chemical, Biological and Explosive Hazards on Surfaces. Micro- and Nanotechnology Sensors, Systems, and Applications Ii 7679. doi:10.1117/12.851785
103. Lopez-Lopez M, Garcia-Ruiz C (2014) Infrared and Raman spectroscopy techniques applied to identification of explosives. TracTrends Anal Chem 54:36–44. doi:10.1016/j.trac.2013.10.011
104. Forest R, Babin F, Gay D, Ho N, Pancrati O, Deblois S, Desilets S, Maheux J (2012) Use of a spectroscopic lidar for standoff explosives detection through Raman spectra. In: Fountain AW (ed) Chemical, Biological, Radiological, Nuclear, and Explosives, vol 8358. Proceedings of SPIE. doi:10.1117/12.918672
105. Ehlerding A, Johansson I, Wallin S, Ostmark H (2012) Resonance-enhanced Raman Spectroscopy on Explosives Vapor at Standoff Distances. International Journal of Spectroscopy: 158715 (158719 pp.)-158715 (158719 pp.). doi:10.1155/2012/158715
106. Ghosh M, Wang L, Asher SA (2012) Deep-Ultraviolet Resonance Raman Excitation Profiles of NH4NO3, PETN, TNT, HMX, and RDX. Appl Spectrosc 66(9):1013–1021. doi:10.1366/12-06626
107. Hug WF, Bhartia R, Sijapati K, Beegle LW, Reid RD (2014) Improved sensing using simultaneous deep-UV Raman and fluorescence detection - II. Chemical, Biological, Radiological, Nuclear, and Explosives (CBRNE) Sensing XV 9073. doi:10.1117/12.2053069
108. Tuschel DD, Mikhonin AV, Lemoff BE, Asher SA (2010) Deep Ultraviolet Resonance Raman Excitation Enables Explosives Detection. Appl Spectrosc 64(4):425–432
109. Yellampalle B, Lemoff BE (2013) Raman Albedo and Deep-UV Resonance Raman Signatures of Explosives. Active and Passive Signatures Iv 8734. doi:10.1117/12.2015951
110. Almaviva S, Angelini F, Chirico R, Palucci A, Nuvoli M, Schnuerer F, Schweikert W, Romolo FS (2014) Eye-safe UV Raman spectroscopy for remote detection of explosives and their precursors in fingerprint concentration. Optics and Photonics for Counterterrorism, Crime Fighting, and Defence X; and Optical Materials and Biomaterials in Security and Defence Systems Technology XI 9253. doi:10.1117/12.2067292
111. Chirico R, Almaviva S, Colao F, Fiorani L, Nuvoli M, Schweiket W, Schnuerer F, Cassioli L, Grossi S, Mariani L, Angelini F, Menicucci I, Palucci A (2014) Proximal detection of energetic materials on fabrics by UV-Raman spectroscopy. Chemical, Biological, Radiological, Nuclear, and Explosives (CBRNE) Sensing XV 9073. doi:10.1117/12.2045572
112. Glimtoft M, Baath P, Saari H, Makynen J, Nasila A, Ostmark H (2014) Towards eye-safe standoff Raman imaging systems. Detection and Sensing of Mines, Explosive Objects, and Obscured Targets XIX 9072. doi:10.1117/12.2049676
113. Akeson M, Nordberg M, Ehlerding A, Nilsson L-E, Ostmark H, Strombeck P (2011) Picosecond laser pulses improves sensitivity in standoff explosive detection. Detection and Sensing of Mines, Explosive Objects, and Obscured Targets XVI 8017. doi:10.1117/12.883351
114. Shreve AP, Cherepy NJ, Mathies RA (1992) Effective rejection of fluorescence interference in Raman spectrosocpy using a shifted excitation difference technique. Appl Spectrosc 46(4):707–711
115. Yellampalle B, McCormick W, Wu H-S, Sluch M, Martin R, Ice R, Lemoff BE (2014) High-sensitivity explosives detection using dual-excitation-wavelength resonance-Raman detector. Chemical, Biological, Radiological, Nuclear, and Explosives (CBRNE) Sensing XV 9073. doi:10.1117/12.2050441
116. Yellampalle B, Sluch M, Asher S, Lemoff B (2011) Multiple-Excitation-Wavelength Resonance-Raman Explosives Detection. Chemical, Biological, Radiological, Nuclear, and Explosives (CBRNE) Sensing XII 8018. doi:10.1117/12.887087
117. Yellampalle B, Sluch M, Wu H-S, Martin R, McCormick W, Ice R, Lemoff BE (2013) Dual-Excitation-Wavelength Resonance-Raman Explosives Detector. Chemical, Biological, Radiological, Nuclear, and Explosives (CBRNE) Sensing XIV 8710. doi:10.1117/12.2015945
118. Moros J, Antonio Lorenzo J, Lucena P, Miguel Tobaria L, Javier Laserna J (2010) Simultaneous Raman Spectroscopy-Laser-induced Breakdown Spectroscopy for Instant Standoff Analysis of Explosives Using a Mobile Integrated Sensor Platform. Anal Chem 82(4):1389–1400. doi:10.1021/ac902470v
119. Moros J, Javier Laserna J (2015) Unveiling the identity of distant targets through advanced Raman-laser-induced breakdown spectroscopy data fusion strategies. Talanta 134:627–639. doi:10.1016/j.talanta.2014.12.001
120. Desilets S, Ho N, Mathieu P, Simard JR, Puckrin E, Theriault JM, Lavoie H, Theberge F, Babin F, Gay D, Forest R, Maheux J, Roy G, Chateauneuf M (2011) Standoff detection of explosives, a challenging approach for optical technologies. Micro- and Nanotechnology Sensors, Systems, and Applications III 8031. doi:10.1117/12.885616
121. Misra AK, Sharma SK, Acosta TE, Porter JN, Lucey PG, Bates DE (2012) Portable standoff Raman system for fast detection of homemade explosives through glass, plastic and water. Chemical, Biological, Radiological, Nuclear, and Explosives (CBRNE) Sensing XIII 8358. doi:10.1117/12.919647
122. Misra AK, Sharma SK, Acosta TE, Porter JN, Bates DE (2012) Single-Pulse Standoff Raman Detection of Chemicals from 120 m Distance During Daytime. Appl Spectrosc 66(11):1279–1285. doi:10.1366/12-06617
123. Ortiz-Rivera W, Pacheco-Londono LC, Castro-Suarez JR, Felix-Rivera H, Hernandez-Rivera SP (2011) Vibrational Spectroscopy Standoff Detection of Threat Chemicals. Micro- and Nanotechnology Sensors, Systems, and Applications Iii 8031. doi:10.1117/12.884433
124. Pettersson A, Wallin S, Ostmark H, Ehlerding A, Johansson I, Nordberg M, Ellis H, Al-Khalili A (2010) EXPLOSIVES STANDOFF DETECTION USING RAMAN SPECTROSCOPY: FROM BULK TOWARDS TRACE DETECTION. Detection and Sensing of Mines, Explosive Objects, and Obscured Targets XV 7664. doi:10.1117/12.852544
125. Wallin S, Pettersson A, Onnerud H, Ostmark H, Nordberg M, Ceco E, Ehlerding A, Johansson I, Kack P (2012) Possibilities for Standoff Raman Detection Applications for Explosives. In: Fountain AW (ed) Chemical, Biological, Radiological, Nuclear, and Explosives, vol 8358. Proceedings of SPIE. doi:10.1117/12.919144
126. Zachhuber B, Ostmark H, Carlsson T (2014) Spatially offset hyperspectral stand-off Raman imaging for explosive detection inside containers. Chemical, Biological, Radiological, Nuclear, and Explosives (CBRNE) Sensing XV 9073. doi:10.1117/12.2053251
127. Almeida MR, Correa DN, Zacca JJ, Lima Logrado LP, Poppi RJ (2015) Detection of explosives on the surface of banknotes by

Raman hyperspectral imaging and independent component analysis. Anal Chim Acta 860:15–22. doi:10.1016/j.aca.2014.12.034
128. Izake EL, Sundarajoo S, Olds W, Cletus B, Jaatinen E, Fredericks PM (2013) Standoff Raman spectrometry for the non-invasive detection of explosives precursors in highly fluorescing packaging. Talanta 103:20–27. doi:10.1016/j.talanta.2012.09.055
129. Petterson IEI, Lopez-Lopez M, Garcia-Ruiz C, Gooijer C, Buijs JB, Ariese F (2011) Noninvasive Detection of Concealed Explosives: Depth Profiling through Opaque Plastics by Time-Resolved Raman Spectroscopy. Anal Chem 83(22):8517–8523. doi:10.1021/ac2018102
130. Dogariu A (2013) Standoff detection and imaging of explosives using CARS. 2013 Conference on Lasers and Electro-Optics
131. Portnov A, Bar I, Rosenwaks S (2010) Highly sensitive standoff detection of explosives via backward coherent anti-Stokes Raman scattering. Appl Phys B-Lasers Optics 98(2–3):529–535. doi:10.1007/s00340-009-3709-3
132. Bremer MT, Wrzesinski PJ, Butcher N, Lozovoy VV, Dantus M (2011) Highly selective standoff detection and imaging of trace chemicals in a complex background using single-beam coherent anti-Stokes Raman scattering. Applied Physics Letters 99 (10). doi:10.1063/1.3636436
133. Moore DS, McGrane SD, Greenfield MT, Scharff RJ (2012) Optimal coherent control methods for explosives detection. Micro- and Nanotechnology Sensors, Systems, and Applications Iv 8373. doi:10.1117/12.920944
134. Moore DS, McGrane SD, Greenfield MT, Scharff RJ, Chalmers RE (2012) Use of the Gerchberg-Saxton algorithm in optimal coherent anti-Stokes Raman spectroscopy. Anal Bioanal Chem 402(1):423–428. doi:10.1007/s00216-011-5348-x
135. Moore DS, Rabitz H, McGrane SD, Greenfield MT, Scharff RJ, Chalmers RE, Roslund J (2011) Optimal Dynamic Detection of Explosives. Chemical, Biological, Radiological, Nuclear, and Explosives (CBRNE) Sensing XII 8018. doi:10.1117/12.882963
136. Bremer MT, Dantus M (2013) Standoff explosives trace detection and imaging by selective stimulated Raman scattering. Applied Physics Letters 103 (6). doi:10.1063/1.4817248
137. Dogariu A, Michael JB, Scully MO, Miles RB (2011) High-Gain Backward Lasing in Air. Science 331(6016):442–445. doi:10.1126/science.1199492
138. Li D-W, Zhai W-L, Li Y-T, Long Y-T (2014) Recent progress in surface enhanced Raman spectroscopy for the detection of environmental pollutants. Microchim Acta 181(1–2):23–43. doi:10.1007/s00604-013-1115-3
139. Upadhyayula VKK (2012) Functionalized gold nanoparticle supported sensory mechanisms applied in detection of chemical and biological threat agents: A review. Anal Chim Acta 715:1–18. doi:10.1016/j.aca.2011.12.008
140. Baker GA, Moore DS (2005) Progress in plasmonic engineering of surface-enhanced Raman-scattering substrates toward ultra-trace analysis. Anal Bioanal Chem 382(8):1751–1770. doi:10.1007/s00216-005-3353-7
141. Hamad S, Podagatlapalli GK, Mohiddon MA, Rao SV (2015) Surface enhanced fluorescence from corroles and SERS studies of explosives using copper nanostructures. Chem Phys Lett 621:171–176. doi:10.1016/j.cplett.2015.01.006
142. Podagatlapalli GK, Hamad S, Mohiddon MA, Rao SV (2014) Effect of oblique incidence on silver nanomaterials fabricated in water via ultrafast laser ablation for photonics and explosives detection. Appl Surf Sci 303:217–232. doi:10.1016/j.apsusc.2014.02.152
143. Jamil AKM, Izake EL, Sivanesan A, Fredericks PM (2015) Rapid detection of TNT in aqueous media by selective label free surface enhanced Raman spectroscopy. Talanta 134:732–738. doi:10.1016/j.talanta.2014.12.022
144. Almaviva S, Botti S, Cantarini L, Fantoni R, Lecci S, Palucci A, Puiu A, Rufoloni A (2014) Ultrasensitive RDX detection with commercial SERS substrates. J Raman Spectrosc 45(1):41–46. doi:10.1002/jrs.4413
145. Almaviva S, Botti S, Cantarini L, Palucci A, Puiu A, Rufoloni A, Landstrom L, Romolo FS (2012) Trace detection of explosives by Surface Enhanced Raman Spectroscopy. Optics and Photonics for Counterterrorism, Crime Fighting, and Defence Viii 8546. doi:10.1117/12.970300
146. Botti S, Cantarini L, Almaviva S, Puiu A, Rufoloni A (2014) Assessment of SERS activity and enhancement factors for highly sensitive gold coated substrates probed with explosive molecules. Chem Phys Lett 592:277–281. doi:10.1016/j.cplett.2013.12.063
147. Botti S, Cantarini L, Palucci A (2010) Surface-enhanced Raman spectroscopy for trace-level detection of explosives. J Raman Spectrosc 41(8):866–869. doi:10.1002/jrs.2649
148. Buettner F, Hagemann J, Wellhausen M, Funke S, Lenth C, Rotter F, Gundrum L, Plachetka U, Moormann C, Strube M, Walte A, Wackerbarth H (2013) Surface Enhanced Vibrational Spectroscopy for the Detection of Explosives. Electro-Optical and Infrared Systems: Technology and Applications X 8896. doi:10.1117/12.2028736
149. Holthoff EL, Stratis-Cullum DN, Hankus ME (2011) A Nanosensor for TNT Detection Based on Molecularly Imprinted Polymers and Surface Enhanced Raman Scattering. Sensors 11(3):2700–2714. doi:10.3390/s110302700
150. Raza A, Saha B (2014) In situ silver nanoparticles synthesis in agarose film supported on filter paper and its application as highly efficient SERS test stripes. Forensic Sci Int 237:E42–E46. doi:10.1016/j.forsciint.2014.01.019
151. Hatab NA, Eres G, Hatzinger PB, Gu B (2010) Detection and analysis of cyclotrimethylenetrinitramine (RDX) in environmental samples by surface-enhanced Raman spectroscopy. J Raman Spectrosc 41(10):1131–1136. doi:10.1002/jrs.2574
152. Mahmoud KA, Zourob M (2013) Fe3O4/Au nanoparticles/lignin modified microspheres as effectual surface enhanced Raman scattering (SERS) substrates for highly selective and sensitive detection of 2,4,6-trinitrotoluene (TNT). The Analyst 138(9):2712–2719. doi:10.1039/c3an00261f
153. Xu Z, Meng X (2012) Detection of 3-nitro-1,2,4-triazol-3-one (NTO) by surface-enhanced Raman spectroscopy. Vib Spectrosc 63:390–395. doi:10.1016/j.vibspec.2012.08.008
154. Zhang C, Wang K, Han D, Pang Q (2014) Surface enhanced Raman scattering (SERS) spectra of trinitrotoluene in silver colloids prepared by microwave heating method. Spectrochim Acta Part A (Mol Biomol Spectrosc) 122:387–391. doi:10.1016/j.saa.2013.11.066
155. Zachhuber B, Carrillo-Carrion C, Simonet Suau BM, Lendl B (2012) Quantification of DNT isomers by capillary liquid chromatography using at-line SERS detection or multivariate analysis of SERS spectra of DNT isomer mixtures. J Raman Spectrosc 43(8):998–1002. doi:10.1002/jrs.3149
156. Talian I, Huebner J (2013) Separation followed by direct SERS detection of explosives on a novel black silicon multifunctional nanostructured surface prepared in a microfluidic channel. J Raman Spectrosc 44(4):536–539. doi:10.1002/jrs.4237
157. Spicer JB, Dagdigian P, Osiander R, Miragliotta J, Zhang XC, Kersting R, Crosley D, Hanson R, Jeffries J (2003) Overview: MURI Center on spectroscopic and time domain detection of trace explosives in condensed and vapor phases. In: Harmon RS, Holloway JH, Broach JT (eds) Detection and Remediation Technologies for Mines and Minelike Targets VIII, Pts 1 and 2, vol 5089. Proceedings of the Society of Photo-Optical Instrumentation Engineers (SPIE). pp 1088–1094. doi:10.1117/12.487531

158. Wojtas J, Mikolajczyk J, Bielecki Z (2013) Aspects of the Application of Cavity Enhanced Spectroscopy to Nitrogen Oxides Detection. Sensors 13(6):7570–7598. doi:10.3390/s130607570
159. Caygill JS, Davis F, Higson SPJ (2012) Current trends in explosive detection techniques. Talanta 88:14–29. doi:10.1016/j.talanta.2011.11.043
160. Taha YM, Odame-Ankrah CA, Osthoff HD (2013) Real-time vapor detection of nitroaromatic explosives by catalytic thermal dissociation blue diode laser cavity ring-down spectroscopy. Chem Phys Lett 582:15–20. doi:10.1016/j.cplett.2013.07.040
161. Wojtas J, Stacewicz T, Bielecki Z, Rutecka B, Medrzycki R, Mikolajczyk J (2013) Towards optoelectronic detection of explosives. Opto-Electronics Rev 21(2):210–219. doi:10.2478/s11772-013-0082-x
162. Snels M, Venezia T, Belfiore L (2010) Detection and identification of TNT, 2,4-DNT and 2,6-DNT by near-infrared cavity ringdown spectroscopy. Chem Phys Lett 489(1–3):134–140. doi:10.1016/j.cplett.2010.02.065
163. Vogelsang M, Welsch T, Jones H (2010) A free-flowing soap film combined with cavity ring-down spectroscopy as a detection system for liquid chromatography. J Chromatogr A 1217(19):3316–3320. doi:10.1016/j.chroma.2009.10.053
164. Harb CC, Boyson TK, Kallapur AG, Petersen IR, Calzada ME, Spence TG, Kirkbride KP, Moore DS (2012) Pulsed quantum cascade laser-based CRDS substance detection: real-time detection of TNT. Opt Express 20(14):15489–15502. doi:10.1364/oe.20.015489
165. Johnson JB, Allen SD, Merten J, Johnson L, Pinkham D, Reeve SW (2014) Standoff Methods for the Detection of Threat Agents: A Review of Several Promising Laser-Based Techniques. J Spectrosc. doi:10.1155/2014/613435
166. Gottfried JL, De Lucia FC, Munson CA, Miziolek AW (2009) Laser-induced breakdown spectroscopy for detection of explosives residues: a review of recent advances, challenges, and future prospects. Anal Bioanal Chem 395(2):283–300. doi:10.1007/s00216-009-2802-0
167. Hahn DW, Omenetto N (2012) Laser-Induced Breakdown Spectroscopy (LIBS), Part II: Review of Instrumental and Methodological Approaches to Material Analysis and Applications to Different Fields. Appl Spectrosc 66(4):347–419. doi:10.1366/11-06574
168. Skvortsov LA (2012) Laser methods for detecting explosive residues on surfaces of distant objects. Quantum Electron 42(1):1–11. doi:10.1070/QE2012v042n01ABEH014724
169. Fortes FJ, Moros J, Lucena P, Cabalin LM, Laserna JJ (2013) Laser-Induced Breakdown Spectroscopy. Anal Chem 85(2):640–669. doi:10.1021/ac303220r
170. Leahy-Hoppa MR, Miragliotta J, Osiander R, Burnett J, Dikmelik Y, McEnnis C, Spicer JB (2010) Ultrafast Laser-Based Spectroscopy and Sensing: Applications in LIBS, CARS, and THz Spectroscopy. Sensors 10(5):4342–4372. doi:10.3390/s100504342
171. Lazic V, Palucci A, Jovicevic S, Carpanese M (2011) Detection of explosives in traces by laser induced breakdown spectroscopy: Differences from organic interferents and conditions for a correct classification. Spectrochim Acta Part B-Atomic Spectrosc 66(8):644–655. doi:10.1016/j.sab.2011.07.003
172. Carter S, Fisher AS, Hinds MW, Lancaster S, Marshall J (2013) Atomic spectrometry update. Review of advances in the analysis of metals, chemicals and materials. J Anal At Spectrom 28(12):1814–1869. doi:10.1039/c3ja90051g
173. Lucena P, Gaona I, Moros J, Laserna JJ (2013) Location and detection of explosive-contaminated human fingerprints on distant targets using standoff laser-induced breakdown spectroscopy. Spectrochim Acta Part B-Atomic Spectrosc 85:71–77. doi:10.1016/j.sab.2013.04.003
174. De Lucia FC, Gottfried JL (2012) Classification of explosive residues on organic substrates using laser induced breakdown spectroscopy. Appl Opt 51(7):B83–B92. doi:10.1364/ao.51.000b83
175. Gottfried JL (2013) Influence of metal substrates on the detection of explosive residues with laser-induced breakdown spectroscopy. Appl Opt 52(4):B10–B19. doi:10.1364/ao.52.000b10
176. Fernandez-Bravo A, Lucena P, Laserna JJ (2012) Selective Sampling and Laser-Induced Breakdown Spectroscopy (LIBS) Analysis of Organic Explosive Residues on Polymer Surfaces. Appl Spectrosc 66(10):1197–1203. doi:10.1366/12-06697
177. Handke J, Duschek F, Gruenewald K, Pargmann C (2011) Standoff Detection Applying Laser-Induced Breakdown Spectroscopy at the DLR Laser Test Range. Chemical, Biological, Radiological, Nuclear, and Explosives (CBRNE) Sensing XII 8018. doi:10.1117/12.886543
178. Wang QQ, Liu K, Zhao H, Ge CH, Huang ZW (2012) Detection of explosives with laser-induced breakdown spectroscopy. Front Phys 7(6):701–707. doi:10.1007/s11467-012-0272-x
179. Delgado T, Vadillo JM, Javier Laserna J (2014) Primary and recombined emitting species in laser-induced plasmas of organic explosives in controlled atmospheres. J Anal At Spectrom 29(9):1675–1685. doi:10.1039/c4ja00157e
180. Sreedhar S, Rao EN, Kumar GM, Tewari SP, Rao SV (2013) Investigation of molecular and elemental species dynamics in NTO, TNT, and ANTA using femtosecond LIBS technique. Chemical, Biological, Radiological, Nuclear, and Explosives (CBRNE) Sensing XIV 8710. doi:10.1117/12.2015685
181. Sreedhar S, Rao EN, Kumar GM, Tewari SP, Rao SV (2013) Molecular formation dynamics of 5-nitro-2,4-dihydro-3H-1,2,4-triazol-3-one, 1,3,5-trinitroperhydro-1,3,5-triazine, and 2,4,6-trinitrotoluene in air, nitrogen, and argon atmospheres studied using femtosecond laser induced breakdown spectroscopy. Spectrochim Acta Part B-Atomic Spectrosc 87:121–129. doi:10.1016/j.sab.2013.05.006
182. Freeman JR, Diwakar PK, Harilal SS, Hassanein A (2014) Improvements in discrimination of bulk and trace elements in long-wavelength double pulse LIBS. Spectrochim Acta Part B-Atomic Spectrosc 102:36–41. doi:10.1016/j.sab.2014.10.008
183. Yang G, Lin QY, Ding Y, Tian D, Duan YX (2015) Laser Induced Breakdown Spectroscopy Based on Single Beam Splitting and Geometric Configuration for Effective Signal Enhancement. Scientific Reports 5. doi:10.1038/srep07625
184. Huang H, Yang L-M, Liu J (2012) Femtosecond fiber-laser-based laser-induced breakdown spectroscopy. In: Fountain AW (ed) Chemical, Biological, Radiological, Nuclear, and Explosives, vol 8358. Proceedings of SPIE. doi:835817 10.1117/12.918615
185. Ahmido T, Ting A, Misra P (2013) Femtosecond laser-induced breakdown spectroscopy of surface nitrate chemicals. Appl Opt 52(13):3048–3057. doi:10.1364/ao.52.003048
186. Bauer AJR, Farrington MP, Sorauf K, Miziolek AW (2014) Laser-induced Breakdown Spectroscopy and Spectral Analysis of Improvised Explosive Materials. Next-Generation Spectroscopic Technologies Vii 9101. doi:10.1117/12.2057930
187. Yang CSC, Brown EE, Hommerich U, Jin F, Trivedi SB, Samuels AC, Snyder AP (2012) Long-Wave, Infrared Laser-Induced Breakdown (LIBS) Spectroscopy Emissions from Energetic Materials. Appl Spectrosc 66(12):1397–1402. doi:10.1366/12-06700
188. Morton KD, Jr., Torrione PA, Collins L (2011) Signal Processing for the Detection of Explosive Residues on Varying Substrates using Laser Induced Breakdown Spectroscopy. Chemical, Biological, Radiological, Nuclear, and Explosives (CBRNE) Sensing XII 8018. doi:10.1117/12.885111

189. Moros J, Serrano J, Sanchez C, Macias J, Laserna JJ (2012) New chemometrics in laser-induced breakdown spectroscopy for recognizing explosive residues. J Anal At Spectrom 27(12):2111–2122. doi:10.1039/c2ja30230f
190. El Haddad J, Canioni L, Bousquet B (2014) Good practices in LIBS analysis: Review and advices. Spectrochim Acta Part B-Atomic Spectrosc 101:171–182. doi:10.1016/j.sab.2014.08.039
191. De Lucia FC, Gottfried JL (2013) Influence of Molecular Structure on the Laser-Induced Plasma Emission of the Explosive RDX and Organic Polymers. J Phys Chem A 117(39):9555–9563. doi:10.1021/jp312236h
192. Serrano J, Moros J, Sanchez C, Macias J, Laserna JJ (2014) Advanced recognition of explosives in traces on polymer surfaces using LIBS and supervised learning classifiers. Anal Chim Acta 806:107–116. doi:10.1016/j.aca.2013.11.035
193. Matroodi F, Tavassoli SH (2014) Simultaneous Raman and laser-induced breakdown spectroscopy by a single setup. Appl Phys B-Lasers Optics 117(4):1081–1089. doi:10.1007/s00340-014-5929-4
194. Moros J, Lorenzo JA, Laserna JJ (2011) Standoff detection of explosives: critical comparison for ensuing options on Raman spectroscopy-LIBS sensor fusion. Anal Bioanal Chem 400(10):3353–3365. doi:10.1007/s00216-011-4999-y
195. Moros J, Laserna JJ (2011) New Raman - Laser induced breakdown spectroscopy identity of explosives using parametric data fusion on an integrated sensing platform. Anal Chem 83:6275–6285. doi:10.1021/ac2009433
196. Moros J, Serrano J, Gallego FJ, Macias J, Laserna JJ (2013) Recognition of explosives fingerprints on objects for courier services using machine learning methods and laser-induced breakdown spectroscopy. Talanta 110:108–117. doi:10.1016/j.talanta.2013.02.026
197. Fortes FJ, Laserna JJ (2010) The development of fieldable laser-induced breakdown spectrometer: No limits on the horizon. Spectrochim Acta Part B-Atomic Spectrosc 65(12):975–990. doi:10.1016/j.sab.2010.11.009
198. Instruments O mPulse. http://www.oxford-instruments.com/products/analysers/handheld-analysers/handheld-libs-mpulse-scrap-metal-analyser
199. LaserSec iLIBS Engine
200. Haisch C (2012) Photoacoustic spectroscopy for analytical measurements. Measurement Science & Technology 23 (1). doi:10.1088/0957-0233/23/1/012001
201. Chien H-T, Wang K, Sheen S-H, Raptis ACP (2012) Photoacoustic Spectroscopy (PAS) System for Remote Detection of Explosives, Chemicals and Special Nuclear Materials. Chemical, Biological, Radiological, Nuclear, and Explosives (CBRNE) Sensing XIII 8358. doi:10.1117/12.919351
202. Chen X, Guo D, Choa FS, Wang CC, Trivedi S, Snyder AP, Ru GJF (2013) Standoff photoacoustic detection of explosives using quantum cascade laser and an ultrasensitive microphone. Appl Opt 52(12):2626–2632. doi:10.1364/ao.52.002626
203. Patimisco P, Scamarcio G, Tittel FK, Spagnolo V (2014) Quartz-Enhanced Photoacoustic Spectroscopy: A Review. Sensors 14(4):6165–6206. doi:10.3390/s140406165
204. Sausa RC, Cabalo JB (2012) The Detection of Energetic Materials by Laser Photoacoustic Overtone Spectroscopy. Appl Spectrosc 66(9):993–998. doi:10.1366/12-06699
205. Bauer C, Willer U, Schade W (2010) Use of quantum cascade lasers for detection of explosives: progress and challenges. Optical Engineering 49 (11). doi:10.1117/1.3498771
206. Choa F-S (2014) Chemical and explosive detections using photoacoustic effect and quantum cascade lasers. Quantum Sensing and Nanophotonic Devices Xi 8993. doi:10.1117/12.2032026
207. Van Neste CW, Liu X, Gupta M, Kim S, Tsui Y, Thundat T (2012) Standoff detection of explosive residues on unknown surfaces. Micro- and Nanotechnology Sensors, Systems, and Applications Iv 8373. doi:10.1117/12.920510
208. Dongkyu L, Seonghwan K, Van Neste CW, Moonchan L, Sangmin J, Thundat T (2014) Photoacoustic spectroscopy of surface adsorbed molecules using a nanostructured coupled resonator array. Nanotechnology 25 (3):035501 (035506 pp.)-035501 (035506 pp.). doi:10.1088/0957-4484/25/3/035501
209. Haupt R (2013) Photoacoustic sensing of explosives.
210. Skvortsov LA, Maksimov EM (2010) Application of laser photothermal spectroscopy for standoff detection of trace explosive residues on surfaces. Quantum Electron 40(7):565–578. doi:10.1070/QE2010v040n07ABEH014334
211. Sharma RC, Kumar D, Bhardwaj N, Gupta S, Chandra H, Maini AK (2013) Portable detection system for standoff sensing of explosives and hazardous materials. Opt Commun 309:44–49. doi:10.1016/j.optcom.2013.06.025
212. Willer U, Schade W (2009) Photonic sensor devices for explosive detection. Anal Bioanal Chem 395(2):275–282. doi:10.1007/s00216-009-2934-2
213. Giubileo G, Colao F, Puiu A (2012) Identification of standard explosive traces by infrared laser spectroscopy: PCA on LPAS data. Laser Phys 22(6):1033–1037. doi:10.1134/s1054660x12060035